

FEASIBILITY OF DEVELOPMENT OF A NUCLEAR DENSITY GAGE
FOR DETERMINING THE DENSITY OF PLASTIC CONCRETE
AT A PARTICULAR STRATUM

FINAL REPORT

BY

DR. FRANK A. IDDINGS
PROFESSOR OF NUCLEAR SCIENCE
LOUISIANA STATE UNIVERSITY

AND

JAMES L. MELANCON
SENIOR SOILS RESEARCH GEOLOGIST
LOUISIANA DEPARTMENT OF TRANSPORTATION AND DEVELOPMENT

Research Report No. FHWA/LA-81/149

State Project No. 736-03-79

Research Project No. 78-1S

Conducted By
LOUISIANA STATE UNIVERSITY
Nuclear Science Center
Baton Rouge, Louisiana

AND

LOUISIANA DEPARTMENT OF TRANSPORTATION
AND DEVELOPMENT
Research and Development Section
In Cooperation With
U. S. Department of Transportation
FEDERAL HIGHWAY ADMINISTRATION

MAY 1981

METRIC CONVERSION CHART

To convert U.S. Units to Metric Units (S.I.), the following conversion factors should be noted:

<u>Multiply U.S. Units</u>	<u>By</u>	<u>To Obtain Metric Units</u>
<u>LENGTH</u>		
inches (in.)	2.5400	centimeters (cm.)
feet (ft.)	0.3048	meters (m.)
yards (yd.)	0.9144	meters (m.)
miles (mi.)	1.6090	kilometers (km.)
<u>AREA</u>		
square inches (in ²)	6.4516	square centimeters (cm ²)
square feet (ft ²)	0.0929	square meters (m ²)
square yards (yd ²)	0.8361	square meters (m ²)
<u>VOLUME</u>		
cubic inches (in ³)	16.3872	cubic centimeters (cm ³)
cubic feet (ft ³)	0.0283	cubic meters (m ³)
cubic feet (ft ³)	28.3162	liters (l.)
cubic yards (yd ³)	0.7646	cubic meters (m ³)
fluid ounces (fl. oz.)	29.57	milliliters (ml.)
gallons (gal.)	3.7853	liters (l.)
<u>MASS (WEIGHT)</u>		
pounds (lb.)	0.4536	kilograms (kg.)
ounces (oz.)	28.3500	grams (g.)
<u>PRESSURE</u>		
pounds per square inch (p.s.i.)	0.07030	kilograms per square centimeters (kg/cm ²)
pounds per square inch (p.s.i.)	0.006894	mega pascal (MPa)
<u>DENSITY</u>		
pounds per cubic yard (lb/yd ³)	0.5933	kilograms per cubic meter (kg/m ³)
bags of cement per cubic yard (cement bags/yd ³)	55.7600	kilograms per cubic meter (kg/m ³)

<u>TEMPERATURE</u>		
degrees fahrenheit (°F.)	5/9 (°F.-32)	degrees celsius (°C.) or centigrade

DISCLAIMER

"The contents of this report reflect the views of the authors who are responsible for the facts and the accuracy of the data presented herein. The contents do not necessarily reflect the official views or policies of the State or the Federal Highway Administration. This report does not constitute a standard, specification, or regulation. Neither the Louisiana State University nor Louisiana Department of Transportation and Development endorse products, equipment or manufacturers. Trade marks or manufacturer's names appear herein only because they are considered essential to the object of this report."

ACKNOWLEDGEMENTS

The authors wish to acknowledge the following persons for their respective efforts during the course of this study: Kirby Shipp, Mike Callihan, Allen B. Causey, Craig Greene and Philip A. Menk, Jr. for the experimental work; Gregory L. Jones and William Hutchison for the preliminary studies; Mitchel Martin and Doug Phillips for core sample density measurements; and Sandra Shipp for assistance with original drawings. The authors also appreciate the editorial contributions of Steve Bokun.

TABLE OF CONTENTS

METRIC CONVERSION CHART -----	iii
ACKNOWLEDGEMENTS -----	v
LIST OF FIGURES -----	iv
LIST OF TABLES -----	xi
ABSTRACT -----	xiii
IMPLEMENTATION STATEMENT -----	xv
INTRODUCTION AND THEORY -----	1
SCOPE -----	5
DESIGN CONSIDERATIONS AND LABORATORY RESULTS -----	7
Transmission -----	7
Backscatter -----	31
FIELD DENSITY RESULTS -----	45
LABORATORY TESTS ON EFFECT OF STEEL REINFORCEMENT -----	47
CONCLUSIONS -----	53
RECOMMENDATIONS -----	57
APPENDICES -----	59
A. Core Scanning Equipment, Procedures and Results -	61
B. Field Density Results -----	75

LIST OF FIGURES

Figure No.	Title	Page No.
5-1	Comparison of Detectors: 2" x 2", 1" x 1", and 3/4" x 1" -----	9
5-2	Effect of Light Pipe Between Crystal and Photomultiplier Tube -----	11
5-3	I_0/I vs. % Air Entrained -----	13
5-4	Radiation Intensity vs. Thickness of Concrete -----	14
5-5	Effect of Concrete Thickness on Gamma Spectrum of Cs-137 Using a 1" x 1" NaI(Tl) Detector -----	15
5-6	Horizontal Scanning Concrete Density Gage -----	17
5-7	Scan Obtained on Concrete Blocks Simulating a Slab-Horizontal Scanning Gage -----	18
5-8	Troxler Model 2376 Density Unit Gage & Calibration Standards -----	19
5-8A	Dual Probe Troxler Gage Modified for Concrete Density -----	20
5-9	Inspection Stand Showing Third "Leg" and Slab Thickness Gage -----	21
5-10	Radiograph of Concrete Block "Y", 99.3lb./cu.ft. ---	23
5-11	Radiograph of Concrete Block "G", 137.7lb/cu.ft. ---	24
5-12	Radiograph of Concrete Block "U", 144.3lb./cu.ft. ---	25
5-13	Radiograph of Concrete Block "R", 115.3lb./cu.ft. ---	26
5-14	Troxler Dual Probe Gage Calibration -----	27
5-15	Percent Change in Count Rates for a Fixed Void Size vs. Path Length -----	29
5-16	Ratio of Change in Count Rate to Standard Deviation vs. Path Length -----	30
5-17	Diagram of Backscatter Gage -----	33
5-18	Source-Detector Shield Design for Backscatter Gage -----	35

LIST OF FIGURES

Figure No.	Title	Page No.
5-19	Gamma Ray Spectra for Backscatter Gage Source-Detector Shield Designs -----	37
5-20	Signal to Noise Ratio vs. Source to Detector Distance -----	38
5-21	Backscatter Gage Measurement on Standard Slabs ----	41
5-22	Backscatter Gage Measurement on Uniform Standard Slab -----	42
5-23	Backscatter Gage Measurement on Non-uniform Stacks of Standard Slabs -----	43
5-24	Calibration Curve for Backscatter Gage with Depth -	44
7-1	The Box and Source/Detector Access Tube Setup for Laboratory Tests of Models -----	49
7-2	A Test Model With Two Rebars Between Source/Detector Access Tubes -----	49
7-3	A Test Model With a Single Rebar Centered Between Source/Detector Access Tubes -----	50
7-4	A Typical Steel Rebar Layout Encountered on a Bridge Deck Tested -----	50
7-5	Plot of Nuclear Density Test Results for Two Layers of Number 5 Rebars With One Bar in Each Layer Between Source and Detector -----	51
7-6	Plot of Nuclear Density Test Results for Two Layers of Number 5 Rebars With Three Bars in Each Layer Between Source and Detector -----	51
7-7	Plot of Nuclear Density Test Results for Laboratory Model With One Number 10 Rebar, Rebar Centered Be- tween Source and Detector -----	52
7-8	Plot of Two Sets of Nuclear Density Tests Results With One Number 10 Rebar, Rebar Placed Near the Source in One Set of Nuclear Readings and Near the Detector in the Other -----	52

LIST OF TABLES

Table	Title	Page No.
5-1	Comparison of Average Density of Concrete Slab Standards vs. Troxler Transmission Gage Measurements -----	28
5-2	Source to Detector Distance Optimization Data -----	39
8-1	Concrete Density Gaging Techniques With Their Advantages and Disadvantages -----	55

Chapter 1

ABSTRACT

Development of a nuclear density gage for determining the degree of consolidation of plastic concrete in selected horizontal layers was determined to be feasible. A commercially available, with some modifications, two-probe density gage (detector in one and source in the other) provided the most reliable laboratory results and is practical for field use. A single probe backscatter gage designed to measure a vertical dimension of plastic concrete demonstrated poor stability and considerable difficulty in calibration. A horizontal scanning technique from pavement edge to pavement edge, measuring the density vertically was studied and determined to be impractical for use.

Densities of plastic concrete were taken on seven construction projects using the two-probe technique. Results are included in the report.

Chapter 2

IMPLEMENTATION STATEMENT

Determination of plastic concrete density through the use of nuclear direct transmission, backscatter and horizontal scanning technique were investigated in this study. Of the three, a dual probe transmission gage was indicated to be the most promising. The dual probe gage, Troxler Model 2376 or similar type manufactured unit, will provide density measurements of selected horizontal layers and can be used in the field with modification of the source-detector unit.

Additional research is recommended to reduce the diameter of both the source and detector tubes. The unit used in this study had 2 inch diameter tubes and one or both could possibly be less without the loss of any design advantages and result in less required effort to push the unit into plastic concrete. Also the full extent of the steel rebar influence on the nuclear readings should be investigated further.

Chapter 3

INTRODUCTION AND THEORY

Introduction

Concrete roadways can fail as the result of voids in the concrete. Voids trapped in the lower layers of the plastic concrete placed in the roadway lead to serious weakening of the slab and are particularly difficult to detect. If the voids, especially those in the lower layers of the concrete slab, could be discovered while the concrete is still plastic, steps can be taken to remove the voids or the defective material and prevent further defective placement. Any disturbance of the plastic concrete by measurements of the consolidation can be repaired by the finishing crew following the placement system. In that regard the consolidation measurement can be considered as non-destructive. Tests made after curing of the concrete, such as coring, are destructive and actually introduce defects into the roadway.

Voids in the concrete may be the result of any one of several factors. Vibrators may be placed incorrectly (too high) or may not be producing proper agitation. The concrete mix may be too dry or may have sat too long in front of the paving machine. The paving machine may move the plastic concrete in a fashion to promote trapping of voids. Even if the above factors are suspected, no tests presently provide an indication of the extent (number, location, and/or size) of the voids left in the pavement.

Some testing for voids has been done using the familiar backscatter soil density gages. These gages can only detect voids in the upper 3 to 4 inches of the slab. Sensitivity for voids drops off rapidly with depth of the void and only voids near the surface are detected. Small voids are not likely to be detected since a large volume of the concrete is involved in the density measurement.

Commercially available backscatter soil density gages are commonly

used in instruments for highway construction but were not designed for void measurement in concrete. If voids occur in the top layer of the concrete, the gage can provide useful information. Another commercially available density gage is the Troxler Model 2376 which uses transmission of gamma rays rather than backscatter for density measurement. This gage permits density measurements of narrow bands or strata vertically through the specimen. Again, the gage was designed for soil density measurements and requires modification for use in plastic concrete.

The work discussed in this report is an evaluation of gages which permit measurement of consolidation in plastic concrete at different depths in the concrete slab, i.e., permit density measurements of strata in the plastic concrete at selected points across the slab.

Theory

There are two ways to set up a gamma radiation source and detector for density measurement. One way uses the transmission of gamma rays. Using the transmission method the source and detector are placed with the specimen between them. For plastic concrete, the source and detector are inside metal tubes. The tubes are then placed in the plastic concrete. As the density of the concrete increases the intensity of the gamma rays reaching the detector decreases. The mathematical relationship relating the intensity of the gamma rays detected to the concrete density (if thickness of the sample between the source and the detector is constant).

$$I = I_0 e^{-\mu_m \rho t} \qquad I = I_0 e^{-(\mu_m t) \rho} \quad (1)$$

I_0 = the intensity of the gamma rays detected when no sample is between the source and detector.

I = the intensity of the gamma rays received by the detector for a certain thickness (t) of the concrete.

ρ = the density of the concrete.

t = thickness of concrete between source and detector.

μ_m = the mass absorption coefficient.

e = a natural mathematical operator.

A second density measuring method is called backscatter. Instead of putting the detector and radioactive source on opposite sides of the sample they are placed on the same side. This method is different from transmission in that instead of the detector receiving the gamma rays that pass through the concrete, the detector receives the gamma rays which are scattered from the concrete. The gamma rays which scatter from the concrete are lower in energy than the rays which are transmitted. This is the result of a process known as Compton scatter.

Compton scatter occurs when part of the energy of the photon is imparted to an electron in an atom. A new photon emerges from the

collision of the original photon and the electron traveling in a new direction with reduced energy.

As the density of the concrete increases, the intensity of the scatter gamma rays reaching the detector increases also. One empirical relationship used for this increase is:

$$I = \rho^a e^{(b + c\rho)} \quad (2)$$

I = the intensity of the gamma rays received by the detector.

ρ = the density of the absorber.

e = a natural mathematical operator.

a,b,&c = empirical values.

The above equation is more difficult to use than the one for transmission. This is because a,b, and c must be experimentally determined and are dependent upon many specimen variables as well as geometry of the source and detector.

Other equations that have been satisfactorily used to model various backscatter gage operations are:

$$I = I_s(1 - e^{-k\rho t}) + I_0 \quad (3)$$

and

$$\frac{I_s - I}{I_s - I_0} = e^{-k\rho t} \quad (4)$$

I = radiation intensity for thickness (t) and density (ρ).

I_s = radiation intensity for an "infinite" product of (t) (ρ).

I_0 = radiation intensity for no specimen present.

k = empirical constant

ρ = density of specimen

t = thickness of specimen

Chapter 4

SCOPE

The objective of this study was to determine the feasibility of development of a portable nuclear density gage for determining the degree of consolidation of plastic concrete at a particular stratum. Two principal gage designs were to be investigated; (1) a two-probe transmission arrangement (source in one and detector in other), (2) a single probe in a depth gage configuration (backscatter). Various gage designs for each test mode were to be evaluated in the laboratory, as well as a manufactured off-the-shelf two-probe transmission gage. After satisfactory performance in the laboratory tests, the most acceptable gage design was to be field tested for portability and ease of operation on concrete paving projects.

CHAPTER 5

Design Considerations and Laboratory Results

Transmission

Design considerations for a transmission gage include: source of radiation, radiation detector and its associated electronics, and source-to-detector geometry. Selection of a radioisotopic source involves characteristics such as half life, energy of emission, availability, and safety. Two radioisotopes that satisfy half life, availability and safety considerations are Cs-137 and Co-60. They are both used now in industrial gages. Radioisotopes such as Ir-192 and Ra-226 were rejected for half life and safety reasons, respectively. Cs-137 has a 30 year half life and a gamma emission of 0.662 MeV while Co-60 has a 5.3 year half life and emits gammas of 1.17 and 1.33 MeV. The long Cs-137 half life is preferred for minimizing calibration frequency and source replacement. The higher gamma energy of the Co-60 was not found to be advantageous as first thought. While the higher energy gammas do penetrate greater thicknesses, reduced sensitivity in the detectors coupled with the large build up of Compton scattered gammas nullified the expected advantage. Therefore, Cs-137 was selected for use in the gage.

Three radiation detectors were considered for use in the gage: ion chamber, GM tube, and scintillation detector. The ion chamber and GM tube detectors have very poor sensitivity for gamma rays, requiring large sources. The ion chamber also requires very expensive electronic circuitry to respond well to the low levels of radiation necessary in portable gages. Only the NaI(Tl) scintillation detector offers high sensitivity, ability to discriminate against scattered radiation, and reasonable cost of the complete counting system. Disadvantages of the scintillation detector are high detector costs, instability, and greater delicacy. However, the disadvantages can be overcome by good instrument design and operating procedures.

While selection of the NaI(Tl) scintillation detector was relatively simple, choice of the size of the detector was not. A large detector provides excellent sensitivity and best discrimination. Figure 5-1 contains gamma spectra obtained with 3 different sizes of NaI(Tl) crystals. These spectra indicate the photopeak (transmitted photon) data loss (poor sensitivity) by the small crystals. The small detector offers easier handling, more localized measurements, better ruggedness and lower cost. The best compromise was found to be a detector having a volume of about 1 cubic inch (16.4 cc). Larger volume detectors were too difficult to handle (insert into plastic concrete) and offer too large a cross section to be able to detect small defects. Good choices are NaI right circular cylinders of either 1 inch diameter by 1 inch height (2.54 cm x 2.54 cm) or 1 1/2 inch diameter by 1/2 inch height (3.81 cm x 1.27 cm).

The two sizes of NaI(Tl) detectors selected offer good sensitivity without excessive source sizes. Sources of from 1 to 10 millicuries (mCi) provide counting rates that give statistically precise measurements in the short times important in plastic concrete testing. Radiation intensities at the detectors should permit accumulation of 10,000 to 50,000 events (counts) to be statistically precise at the 68% confidence level of a standard deviation of 1% or better. The radiation intensity of the non-shielded sources of 1 to 10 mCi present no safety hazard to personnel using the gages. A 1 mCi Cs-137 source produces a radiation intensity of 3.3 milliroentgens per hour (mr/hr) at 1 foot from the source in air. Personnel radiation exposures must be kept below an average of 100 mr per week. With the 1 to 10 mCi sources of Cs-137, personnel radiation exposures are easily kept below the 100 mr/week limit. Typical personnel exposures using a 5 mCi Cs-137 source in a gage were from 0 (undetectable) to 3 mr in 1 day of continuous field work.

The 1 inch x 1 inch NaI(Tl) crystal has not worked well in most of the field studies reported here while the laboratory studies looked excellent. To use the 1 inch x 1 inch crystal, a plastic "light

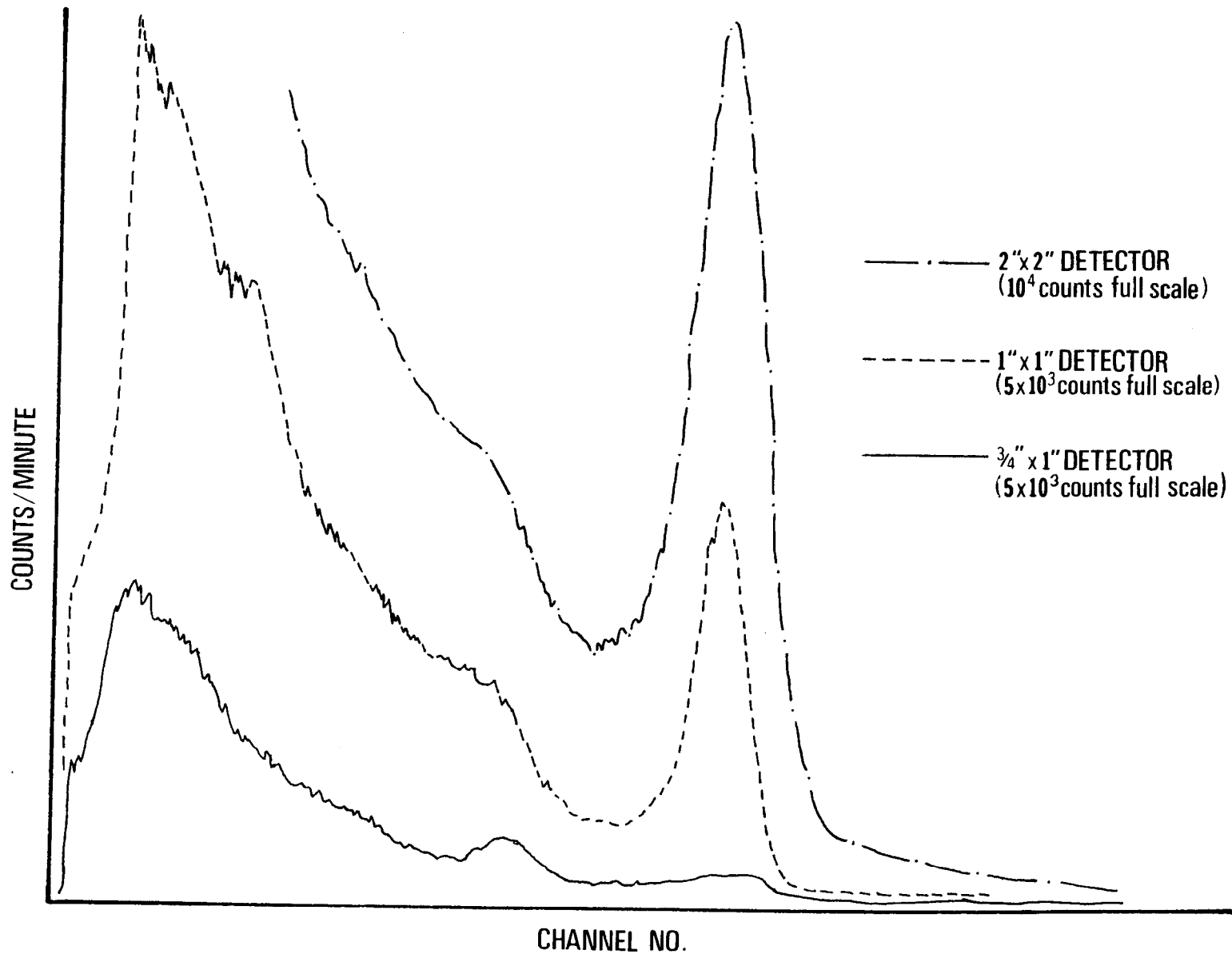


Figure 5-1
COMPARISON OF DETECTORS

pipe" had to be used to connect the crystal to the 2 inch diameter photomultiplier tube - preamplifier electronic systems available. This coupling system lost some of the sensitivity, resolution, discrimination, and ruggedness inherent in the 1 inch x 1 inch detector system (without the light pipes). Figure 5-2 consists of two gamma spectra accumulated using a 1 inch x 1 inch NaI(Tl) crystal mounted directly to a 2 inch diameter photomultiplier tube and with an acrylic plastic light pipe 8 inches long x 1 1/4 inches diameter. With matching photomultiplier and preamplifier systems of 1 inch diameter, the 1 inch x 1 inch detector will offer considerable advantage over the 1/2 inch thick x 1 1/2 inches diameter NaI(Tl) detector system found to be most satisfactory. The 1/2 inch x 1 1/2 inches detector system is a commercially packaged system with considerable ruggedness.

Electronics necessary for the scintillation detector systems include a stable high voltage power supply (900 VDC+), a linear amplifier for the preamplified pulses, a pulse height analyzer or single channel analyzer, scaler, and timer. The pulse height analyzer uses a variable electronic gate to reject pulses lower than a selected amplitude. A single channel analyzer uses two variable electronic gates to select a narrow range of pulse amplitudes (related to gamma energy absorption in the detector crystal). The scaler digitally sums the events of selected amplitude detected in the time interval set with the timer. All of the above components can be contained in a small, battery powered system such as the Troxler Model 2376 or the Eberline Model MS-1. For early laboratory studies, individual components were assembled and often used in conjunction with multichannel analyzers to observe all energy regions rather than the single value available from a scaler system.

Once the detector and source were chosen, their relative positioning, or geometry, was the next consideration. For transmission gages, theoretical considerations predict a relationship between the absorption coefficient and the product of density-thickness to obtain optimum sensitivity:

$$\mu_m \rho t = 2 \quad (5)$$

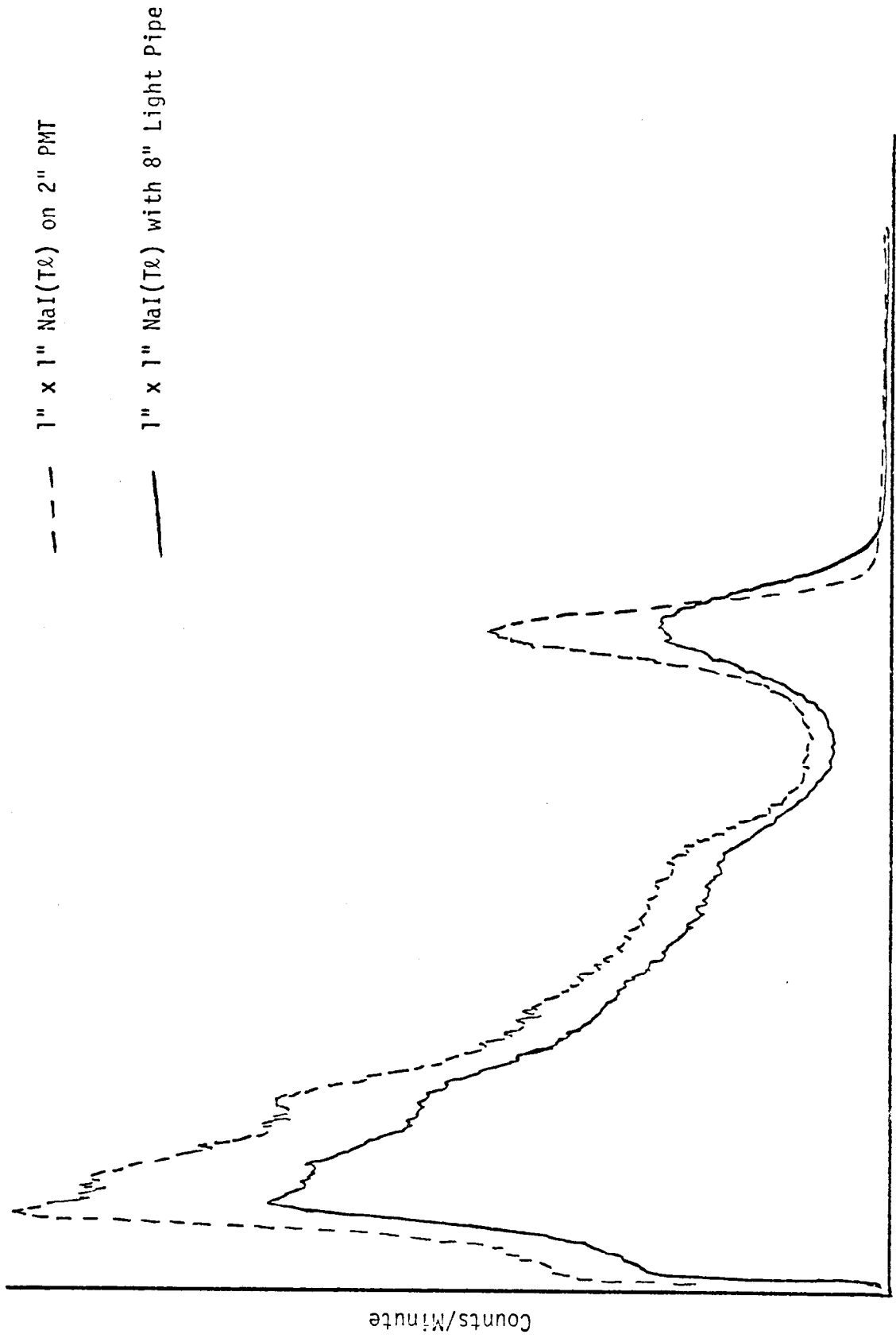


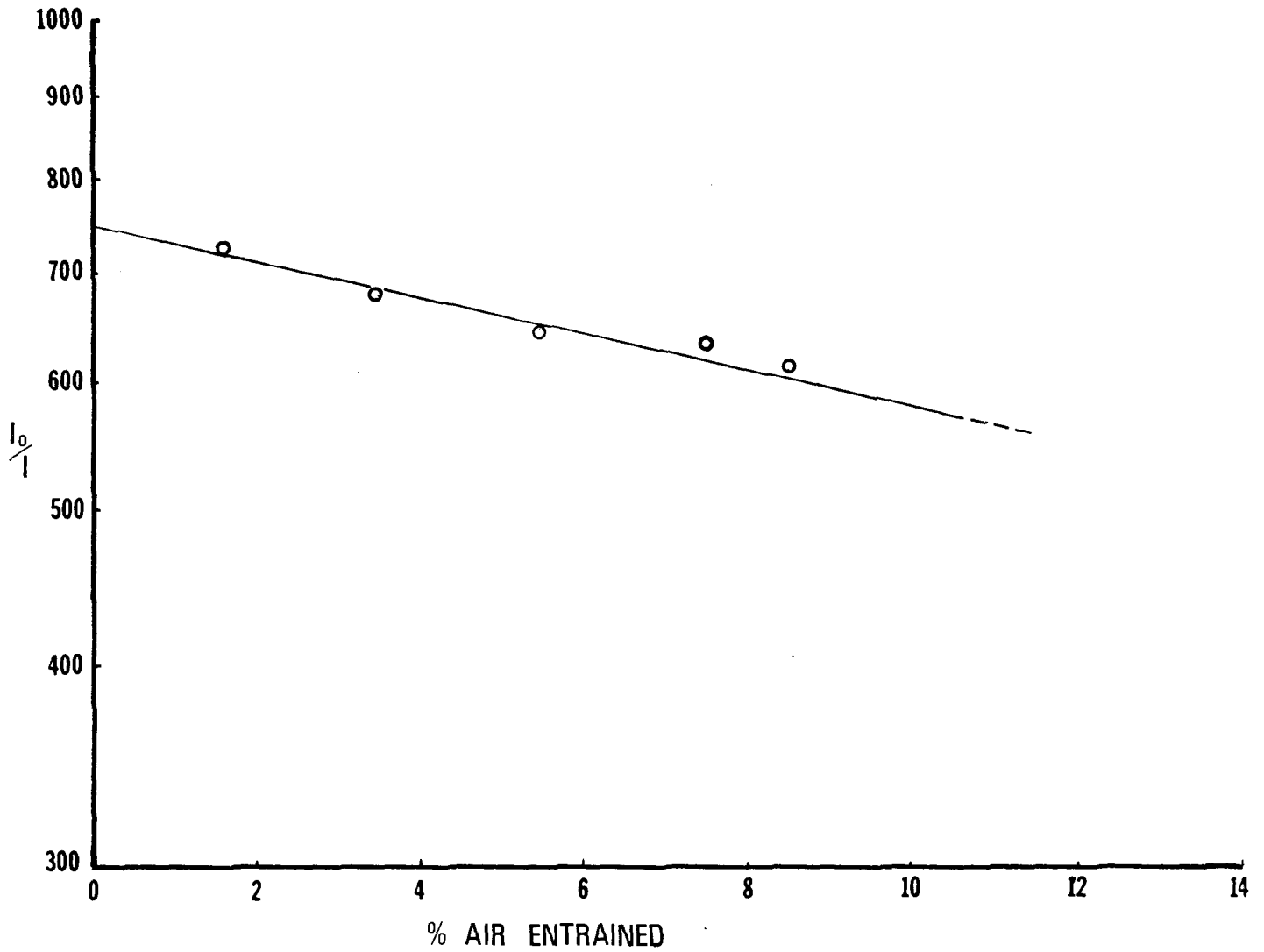
Figure 5-2

EFFECT OF LIGHT PIPE BETWEEN SCINTILLATION CRYSTAL AND PHOTOMULTIPLIER TUBE

$$\mu_m \rho t = 2$$

For Cs-137, the μ_m is approximately $0.099 \text{ cm}^2/\text{g}$ for the components making up concrete (μ_m for Al is $0.074 \text{ cm}^2/\text{g}$ and μ_m for water is $0.086 \text{ cm}^2/\text{g}$). An average density for concrete may be taken as $\sim 2 \text{ g/cc}$ (for 136 lb/cu.ft). Optimum thickness of concrete for the gage using Cs-137 would be 12.5 cm or 5 inches . Thicknesses larger than 5 inches will give better sensitivity at the expense of count rate. This optimization appears to be correct in that per cent air entrainment in concrete cylinders of diameter 12.7 cm (5 inches) could be determined as shown in Figure 5-3. The excellent relationship between radiation intensity and thickness of concrete for a wide range of thicknesses may be illustrated by plots such as Figure 5-4. While measurements of density may be made with radiation path lengths much greater than 5 inches , much longer counting times are required and the transmitted photon information required and the transmitted photon information (photopeak) in gamma spectrum obtained is badly degraded. Figure 5-5 allows comparison of gamma spectra made with $1 \text{ inch} \times 1 \text{ inch}$ NaI(Tl) crystal and $1 \frac{1}{2} \text{ mCi}$ Cs-137 source across increasing thicknesses of concrete of uniform density. The separation of source and detector must be large enough to inspect a reasonable amount of the concrete. The 12 inches separation used in the Troxler Model 2376 appears to be maximum practical for sensitivity enough to detect a small void with adequate photopeak data being detected while encompassing a reasonable fraction of the total slab width. Path lengths of over 24 inches can be measured but the source sizes became impractical, even hazardous, to handle.

The long path lengths were examined to determine if a large source could be inserted into the plastic concrete and then the detector could be moved vertically at the edge of the slab while only the source is moved in a tube in the concrete. No advantage for this geometry was obtained and long enough path lengths to inspect far enough across the slab (at least half-way) could not be obtained with practical sources.



EBERLINE MS-1 USED WITH 2 INCH NaI(Tl) CRYSTAL. SIX SECOND
 COUNTING TIME, WINDOW OUT, THRESHOLD 3.59, H.V. 7.6, 12.7cm
 TRANSMISSION DISTANCE THROUGH CONCRETE SAMPLES. 1mCi
 Cs 137 SOURCE

Figure 5-3

I_0/I vs. % AIR ENTRAINED

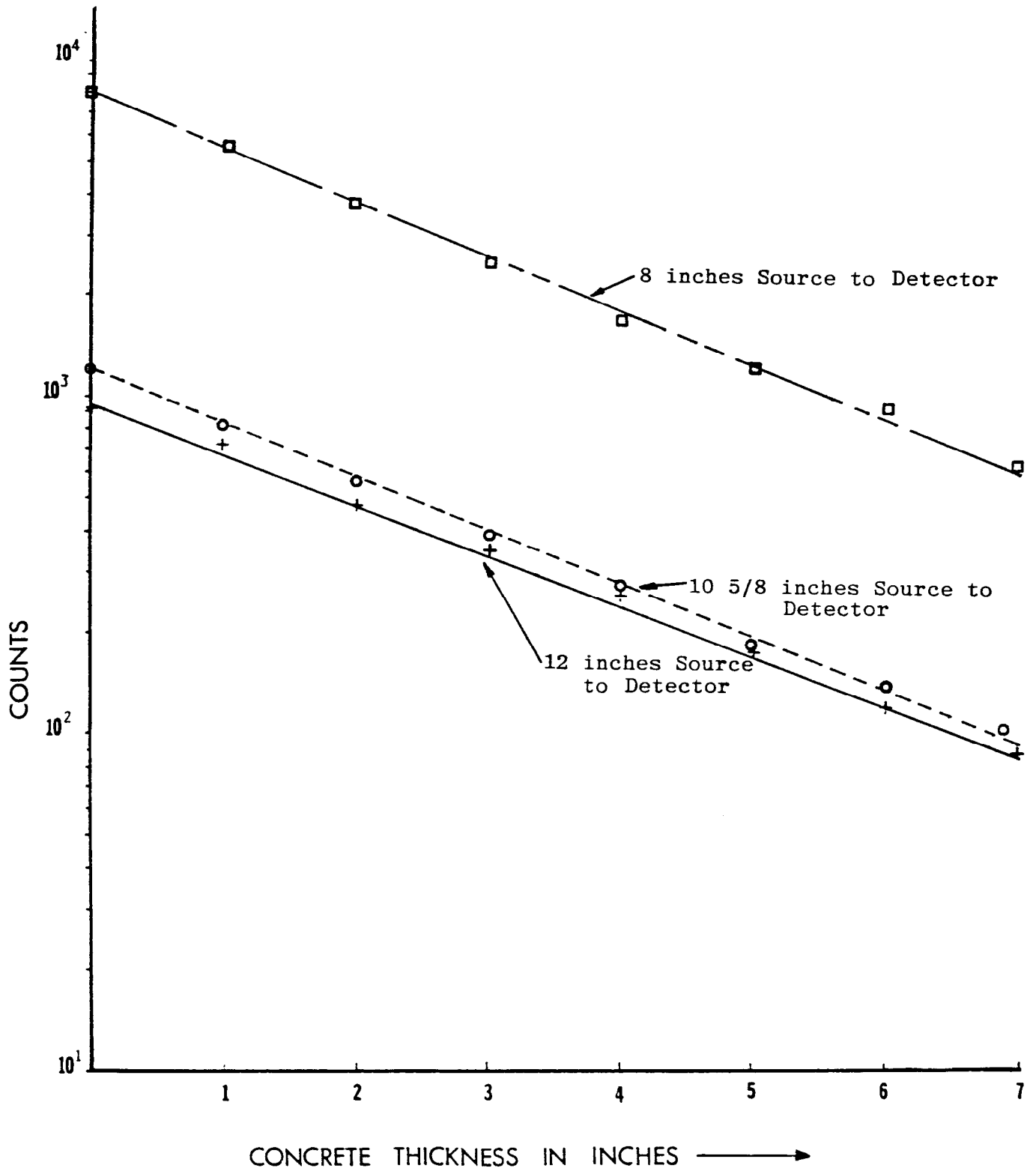
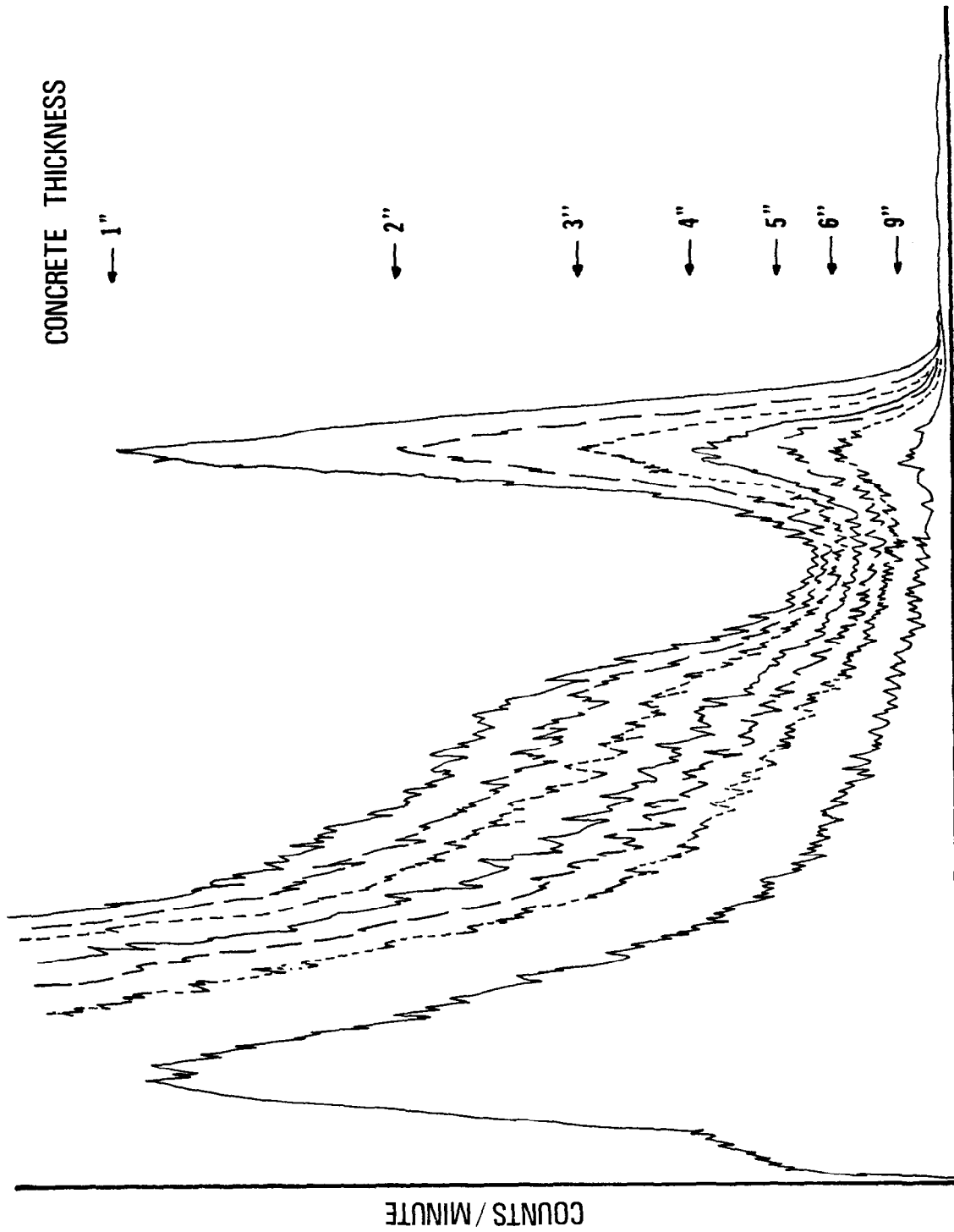


Figure 5-4
 RADIATION INTENSITY VS THICKNESS OF CONCRETE



EFFECT OF CONCRETE THICKNESS ON GAMMA SPECTRUM OF Cs-137
 USING A 1"x1" NaI(Tl) DETECTOR

Figure 5-5

Another geometry considered is the vertical radiation path with placement of the source and detector across the thickness of the concrete slab. This may be done by placing small tubes on or in the base in front of the paving machine. After the placement of the plastic concrete, the small Cs-137 source is moved through a tube with a wire while a detector moves above the surface of the slab immediately above the source. The source and detector move together when pulled by wires attached to pulleys on the same shaft. In this fashion, the entire width of the slab at a particular point can be scanned. This method does not give a vertical location of voids but does detect any voids between the bottom and surface of the slab as well as any other discontinuities such as rebar. Figure 5-6 is a sketch of the scanning system devised and Figure 5-7 is the scan obtained on concrete blocks stacked to simulate a slab with changes in density, voids, and rebar. No field studies of this system, which is outside the scope of the original contract, were conducted.

Another auxiliary scanning study conducted to assist in this research project was the design, construction and use of a gage to scan concrete core samples. A description of that equipment and results are in Appendix A.

The Troxler Model 2376 density gage source detector system, Figure 5-8, was modified to permit its use in plastic concrete as shown in Figure 5-8A. A third "leg" in the form of a moveable 1/2 inch diameter aluminum rod was added to the inspection stand, as shown in Figure 5-9. The third leg provides better vertical positioning of the source-detector tubes in the plastic concrete. Points were also added to the 2 inches diameter source and detector tubes to ease insertion into the plastic concrete as well as to keep the water and concrete out of the tubes.

For laboratory studies of equipment, geometric parameters, and sensitivity, sets of standard concrete blocks were prepared. The first set was 1 inch (2.54cm) thick and the second set was 2 inches

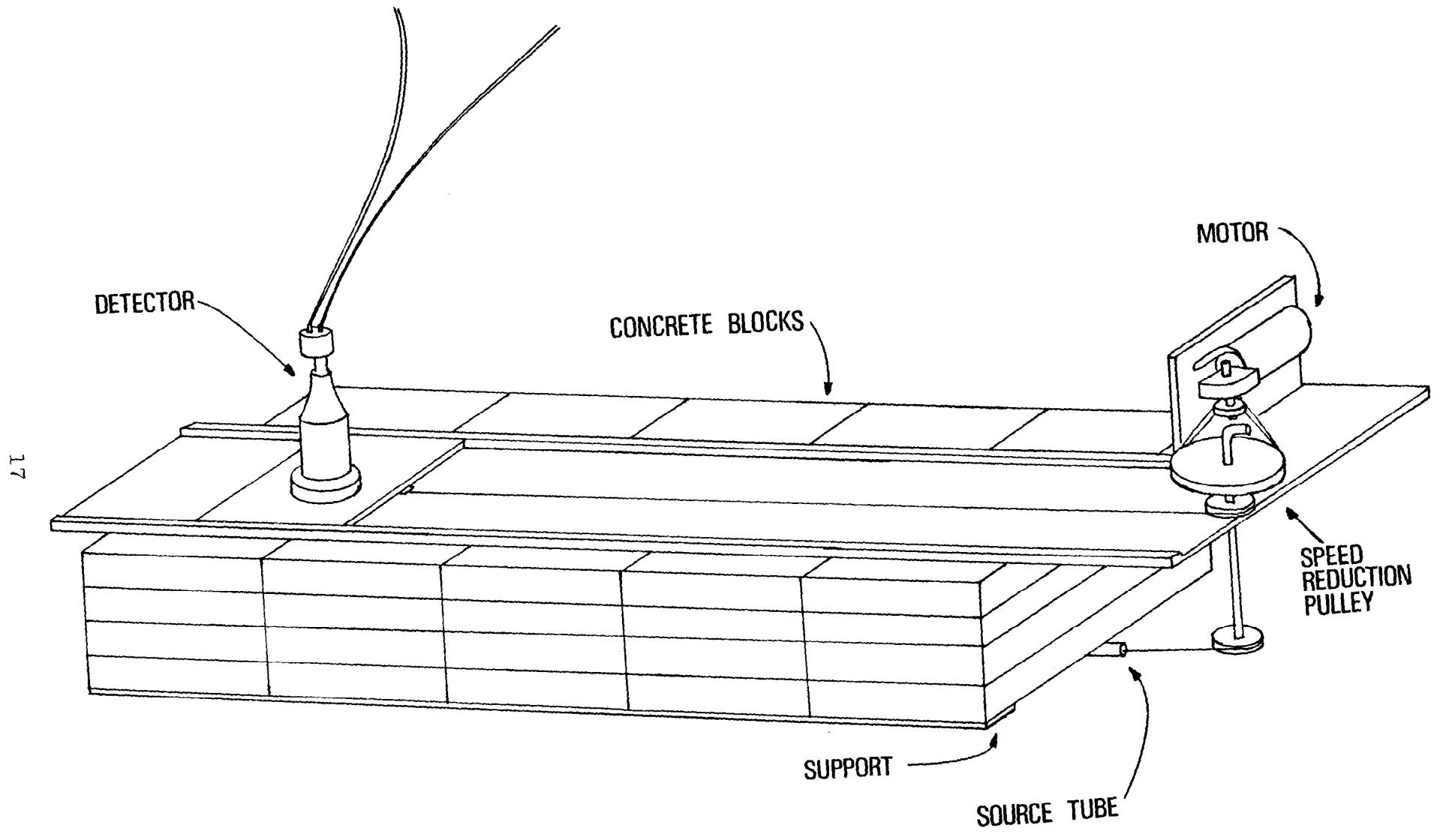


Figure 5-6
HORIZONTAL SCANNING CONCRETE DENSITY GAGE

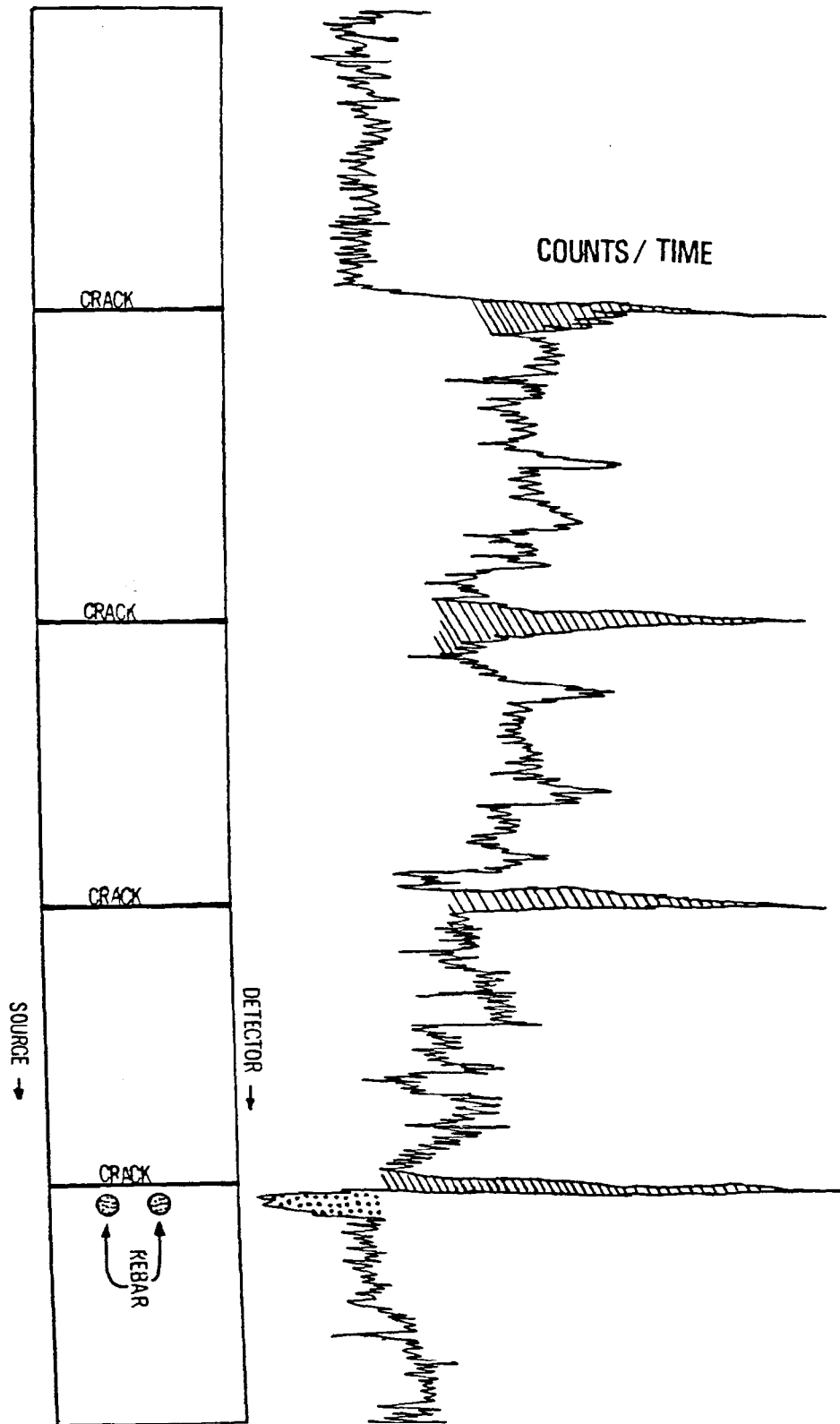


Figure 5-7

SCAN OBTAINED ON CONCRETE BLOCKS SIMULATING A SLAB

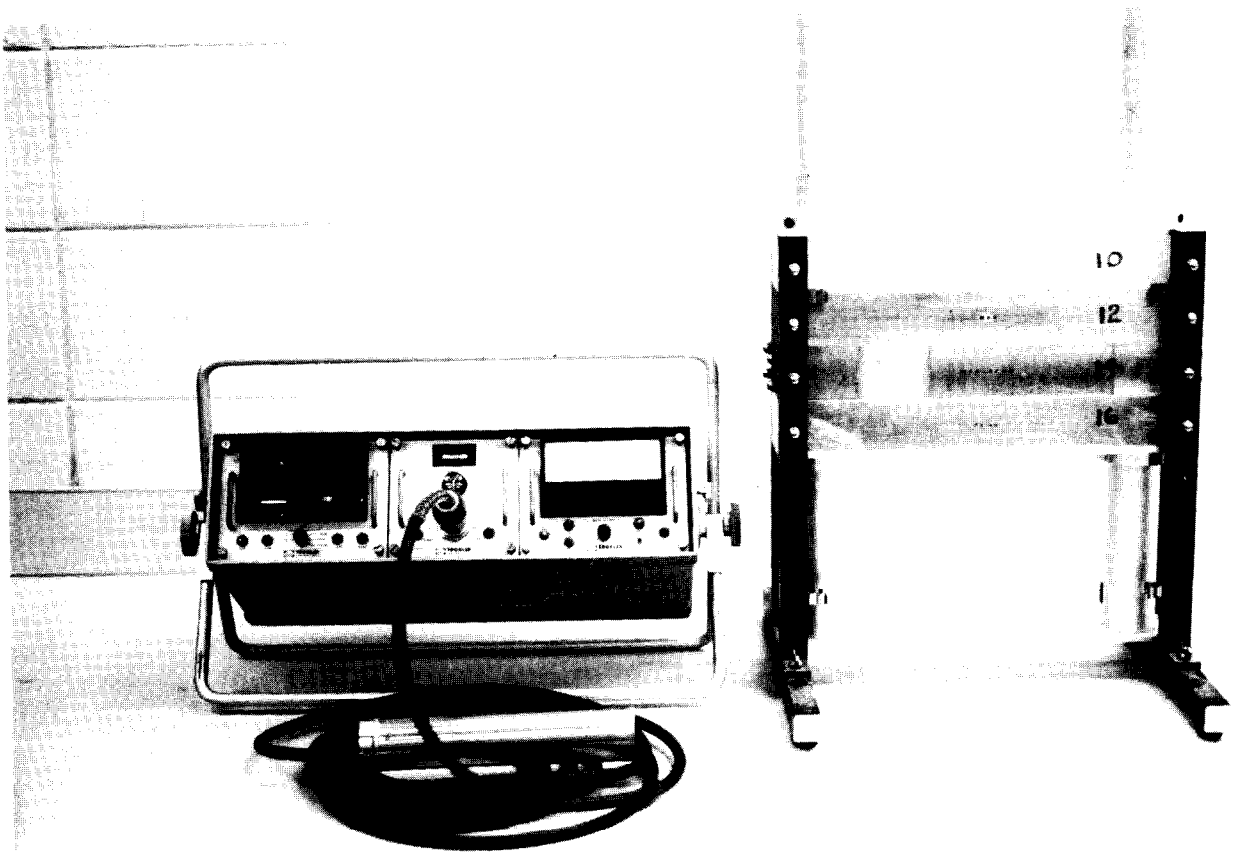


Figure 5-8

TROXLER MODEL 2376 DENSITY GAGE & CALIBRATION STANDARDS

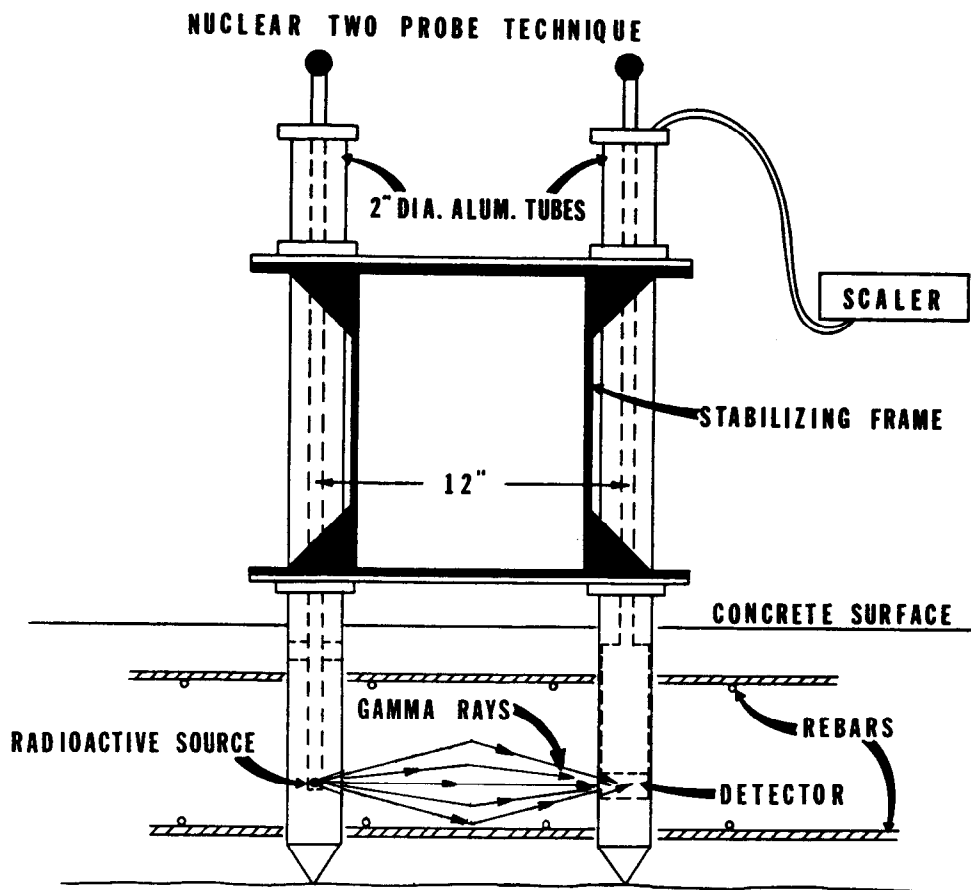


Figure 5-8A

TROXLER TWO PROBE SYSTEM MODIFIED FOR USE IN PLASTIC CONCRETE

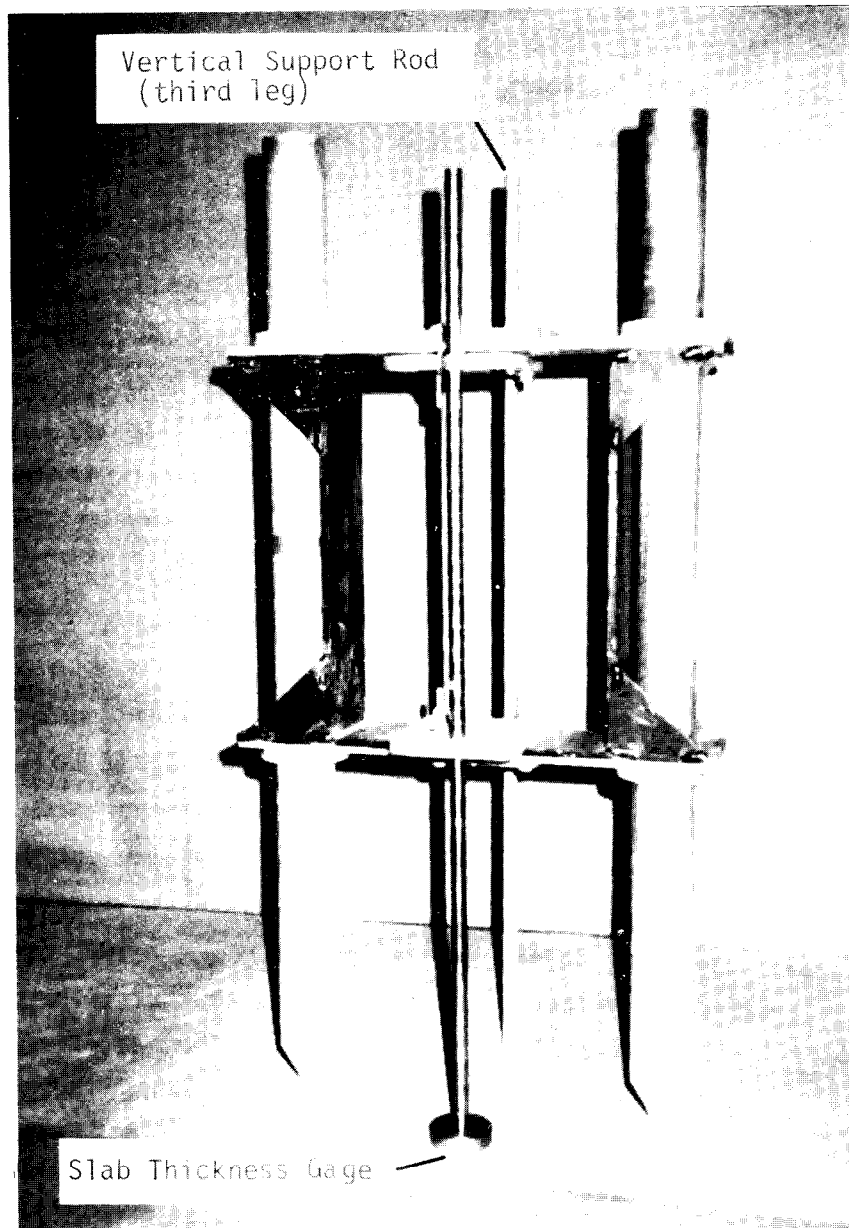


Figure 5-9

INSPECTION STAND SHOWING THIRD "leg" AND SLAB THICKNESS GAGE

(5.08 cm) thick. The second set had two 2 inch diameter holes spaced on 12 inch centers to accommodate the Troxler Model 2376 density probes. The concrete slabs had calculated densities (total weight/measured volume) of from 99 to 145 pounds per cubic foot. The range of densities was obtained by using different aggregates including crumbled styrofoam. Average (calculated) densities varied from densities measured by radiation gage for some of the blocks. These results could be explained by non-uniform density sections in those blocks between the holes for the density probes. The non-uniform density areas can be seen in radiographs of those blocks giving erratic data. Figures 5-10 through 5-13 are copies of selected radiographs of the area between the two probe holes for several of the standard concrete blocks.

Figure 5-14 is a plot of count rate versus density for several standard concrete blocks as well as four Troxler standard blocks (polyethylene, magnesium, magnesium-aluminum, and aluminum). The plot exhibits the excellent results possible with the transmission gage. Table 5-1 allows comparison of results from the transmission gage with calculated density and with another research group in another laboratory. As expected from the radiographic study of the blocks, some give the expected density by transmission gaging and others do not. The agreement between the results of the two different laboratory groups is excellent. Repetitions over periods of several months also gave excellent agreement indicating excellent stability of instrumentation and reproducibility of results.

Figures 5-15 and 5-16 provide an indication of percent change in count rate and the ratio of change in count rate to standard deviation of count for increasing thicknesses of concrete for 1 inch and 1/2 inch voids. As expected, the voids become more difficult to detect as thickness increases but are still detectable even at a path length of 12 inches of concrete.

Figure 5-16 is the more important of the two figures. As long

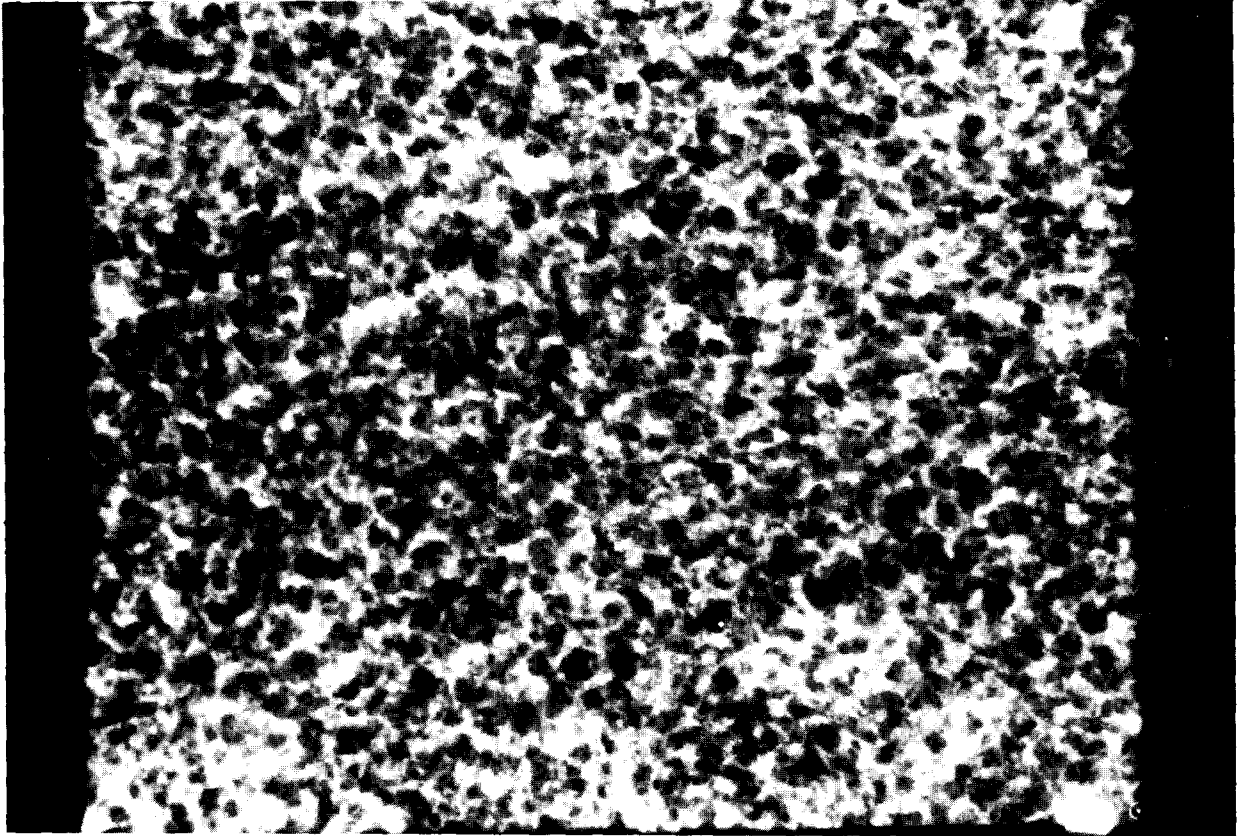


Figure 5-10

RADIOGRAPH OF CONCRETE BLOCK "Y"
100% LIGHT WEIGHT AGGREGATE, 99.31b/cu.ft.

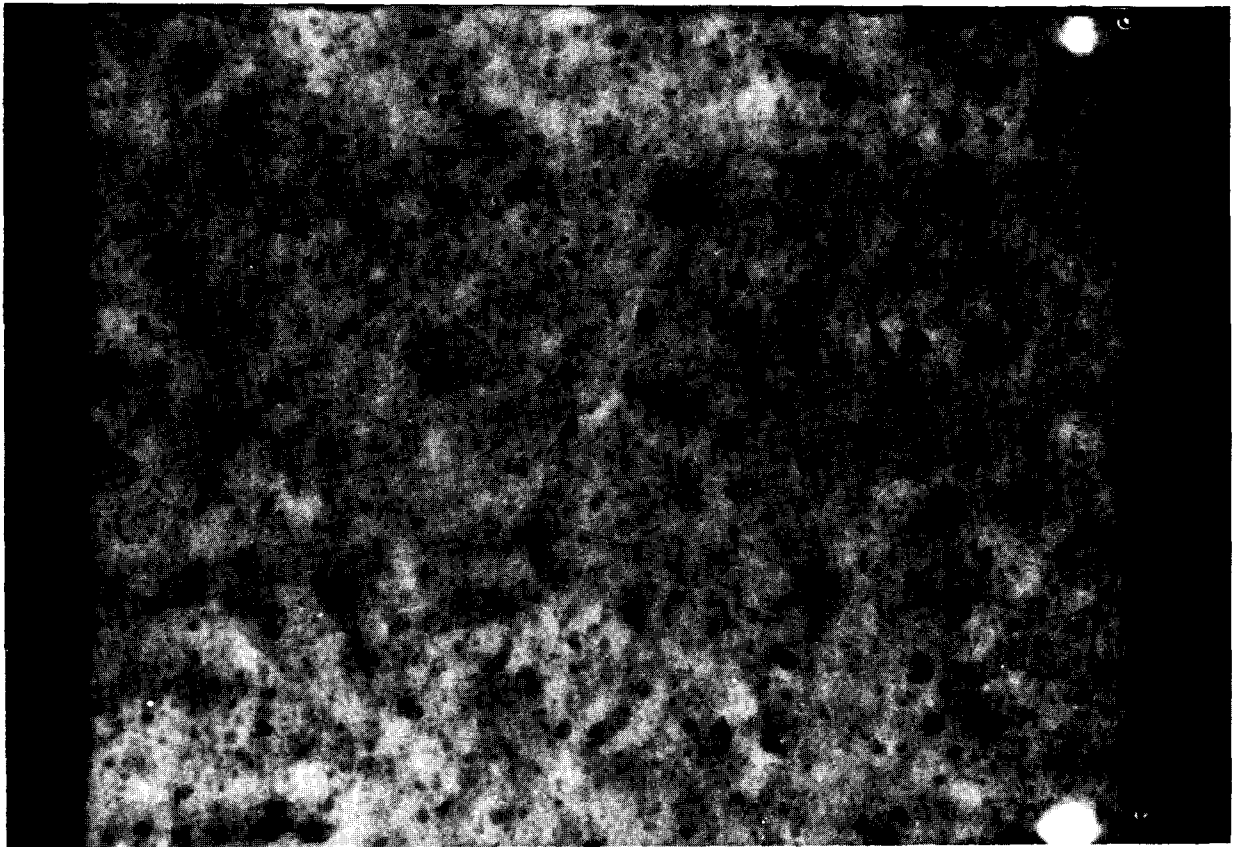


Figure 5-11

RADIOGRAPH OF CONCRETE BLOCK "G"
NORMAL SAND/GRAVEL MIXTURE, 137.7lb/cu.ft.

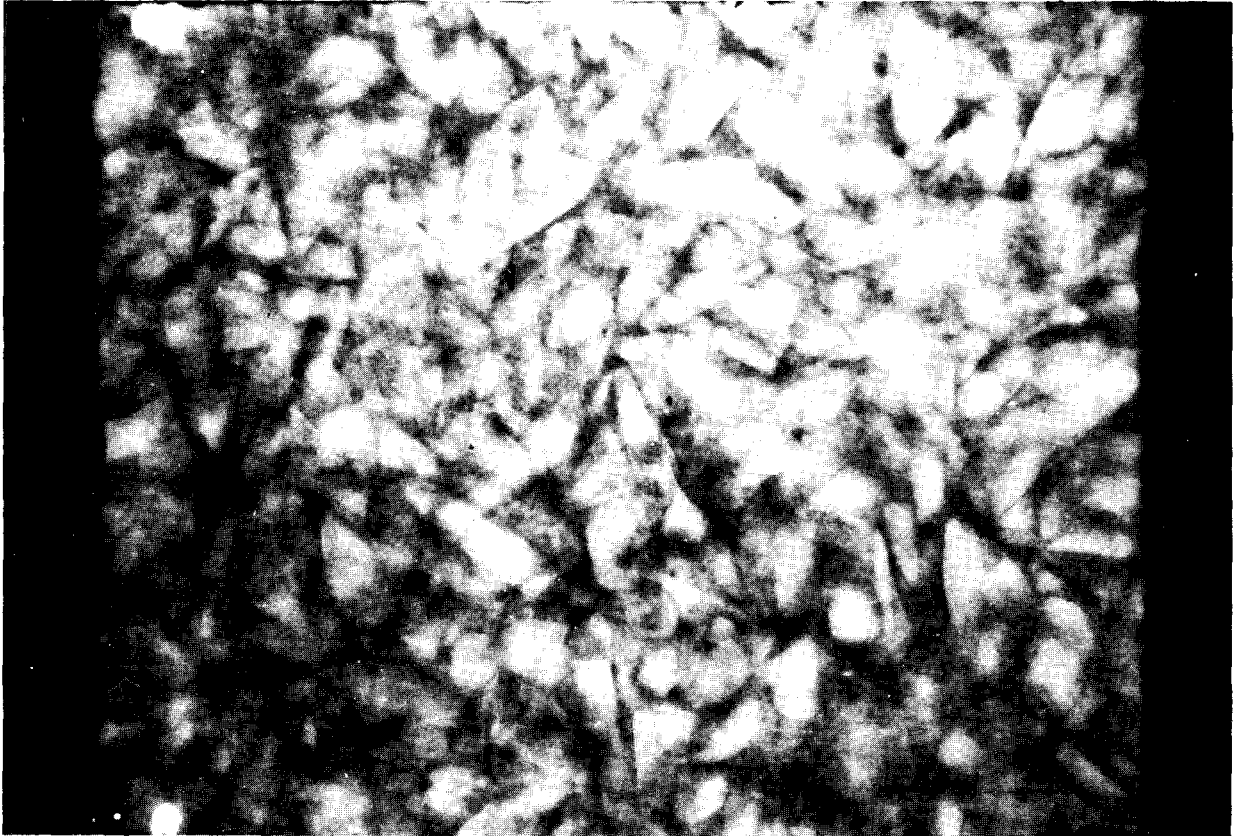


Figure 5-12

RADIOGRAPH OF CONCRETE BLOCK "U"
100% LIMESTONE AGGREGATE, 144.31b/cu.ft.

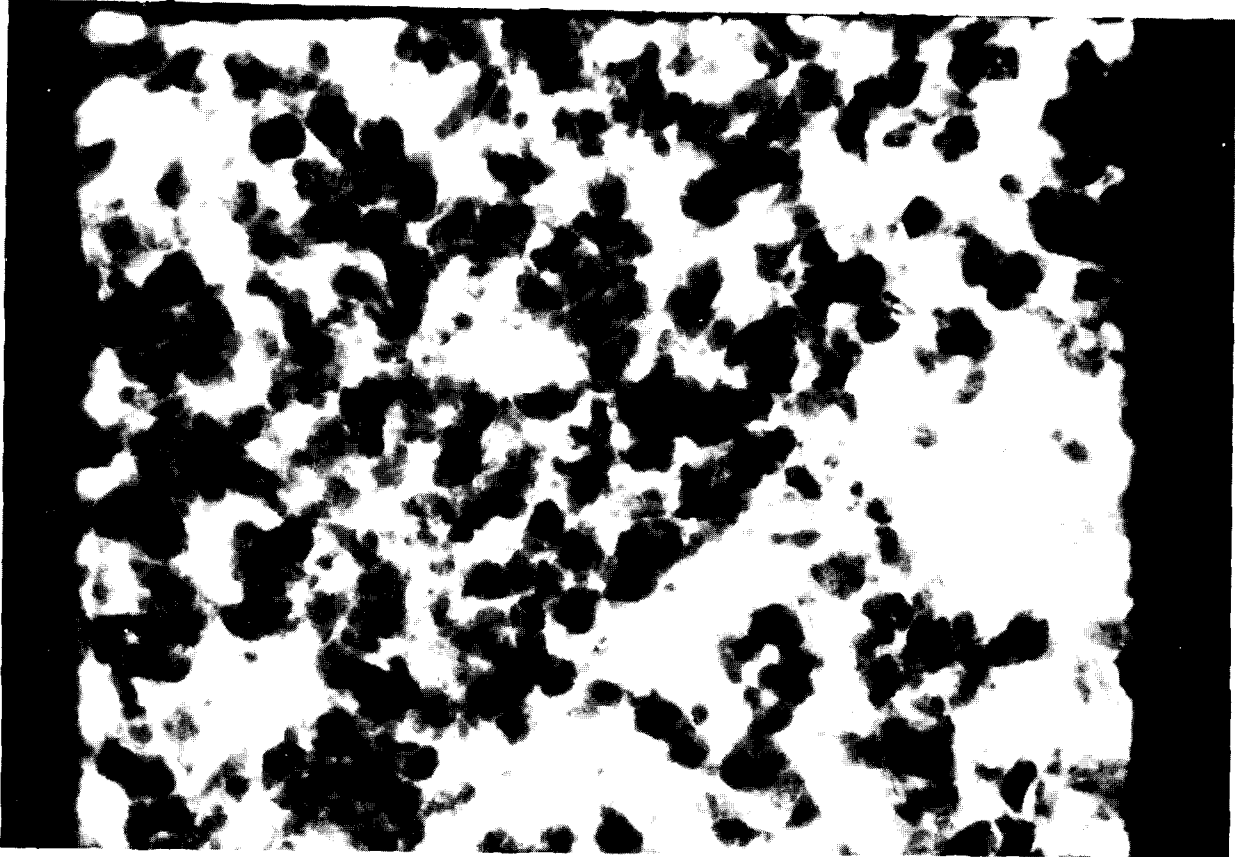


Figure 5-13

RADIOGRAPH OF CONCRETE BLOCK "R"

50/50 Styrofoam-Gravel as Aggregate, 115.3 lb/cu. ft.
Average density and density across center of block
will not match because of the large high density area
on the right side of radiograph.

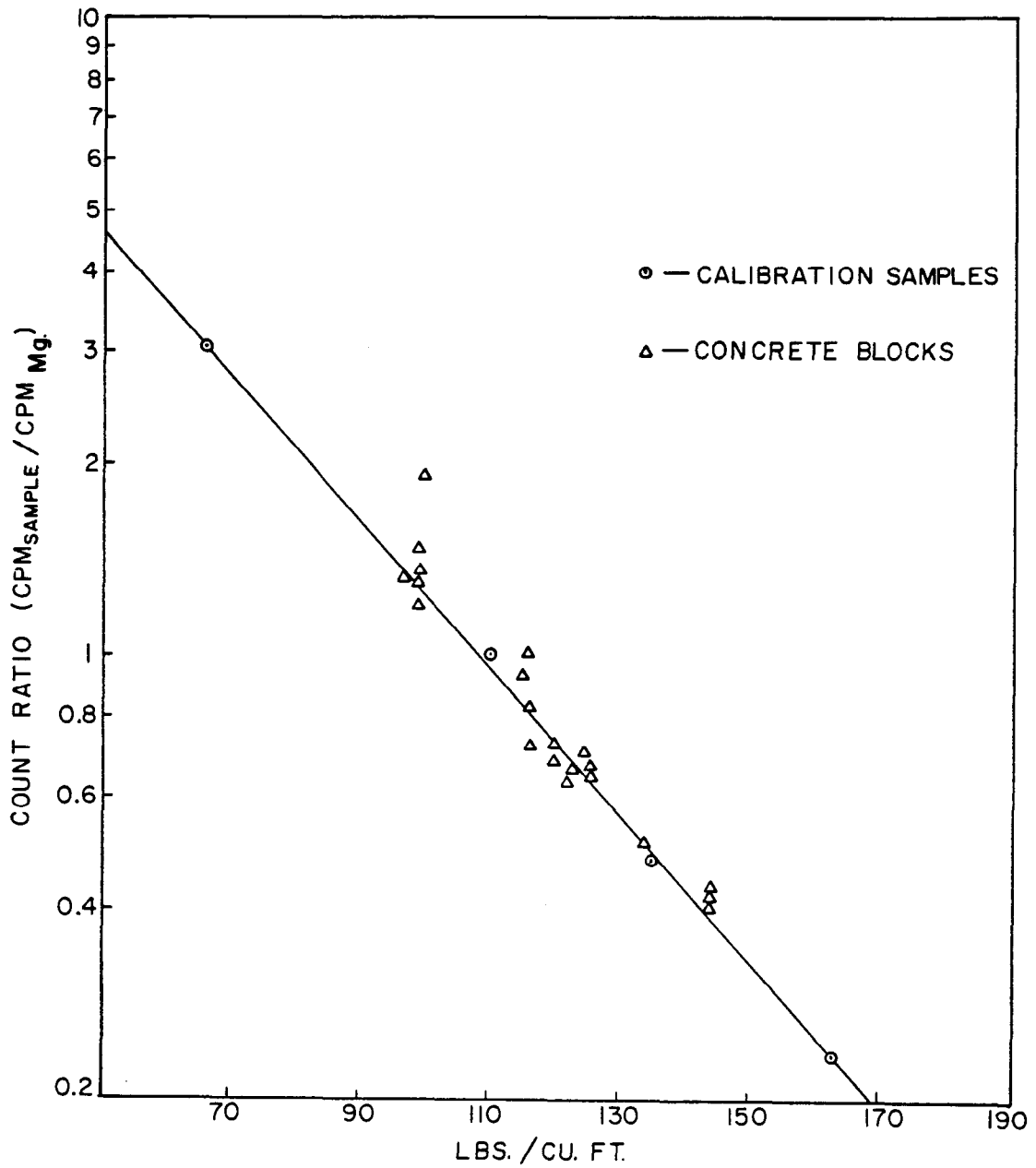


Figure 5-14

Troxler Count Rate Versus Density for Several Lab Standard Concrete Blocks and for the Four Troxler Calibration Standards

Table 5-1

Comparison of Average Density of Concrete Slab Standards
vs. Troxler Transmission Gage Measurements

Slab ¹	Calculated Density ²	Nuclear Density ²	
		Group 1	Group 2
A	136.5	135.8	136.0
B	134.8	131.5	133.4
C	135.2	132.0	132.1
D	135.3	131.8	131.2
E	106.8	101.8	98.9
F	135.5	134.8	135.6
G	137.7	136.2	136.2
H	134.4	131.2	131.5
I	119.4	113.8	111.9
J	133.9	133.6	133.8
K	134.9	--	--
L	135.1	134.8	135.6
M	99.4	95.0	
N	99.1	97.5	
O	99.3	94.0	
P	100.4	83.5	
Q	116.3	107.5	
R	115.3	--	
S	115.7	111.5	
T	117.3	92.0	
U	144.3	144.0	
V	144.3	147.0	
W	144.1	141.5	
X	144.4	144.5	
Y	99.3	95.8	
Z	97.7	97.5	
AA	99.3	99.0	
AB	99.3	97.0	
AC	122.4	127.0	
AD	116.3	120.0	
AE	116.0	122.0	
AF	119.8	121.5	
AG	125.4	122.0	
AH	123.7	125.0	
AI	126.8	125.5	
AJ	124.4	126.0	

1 - 2 X 12 X 22 inches

2 - Density in pounds per cubic feet

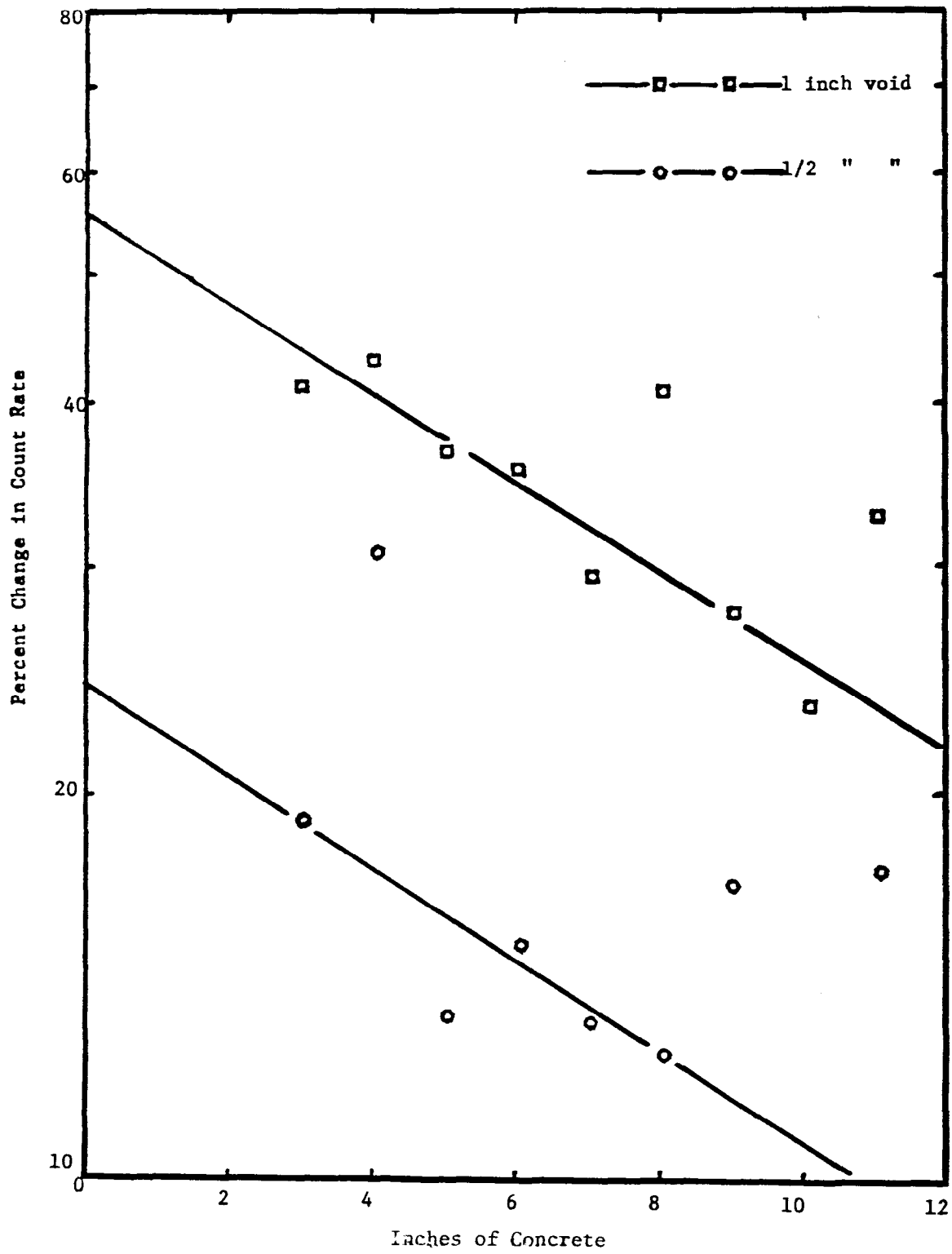


Figure 5-15
 PERCENT CHANGE IN COUNT RATE FOR A FIXED VOID SIZE FOR
 DIFFERENT PATH LENGTHS IN CONCRETE

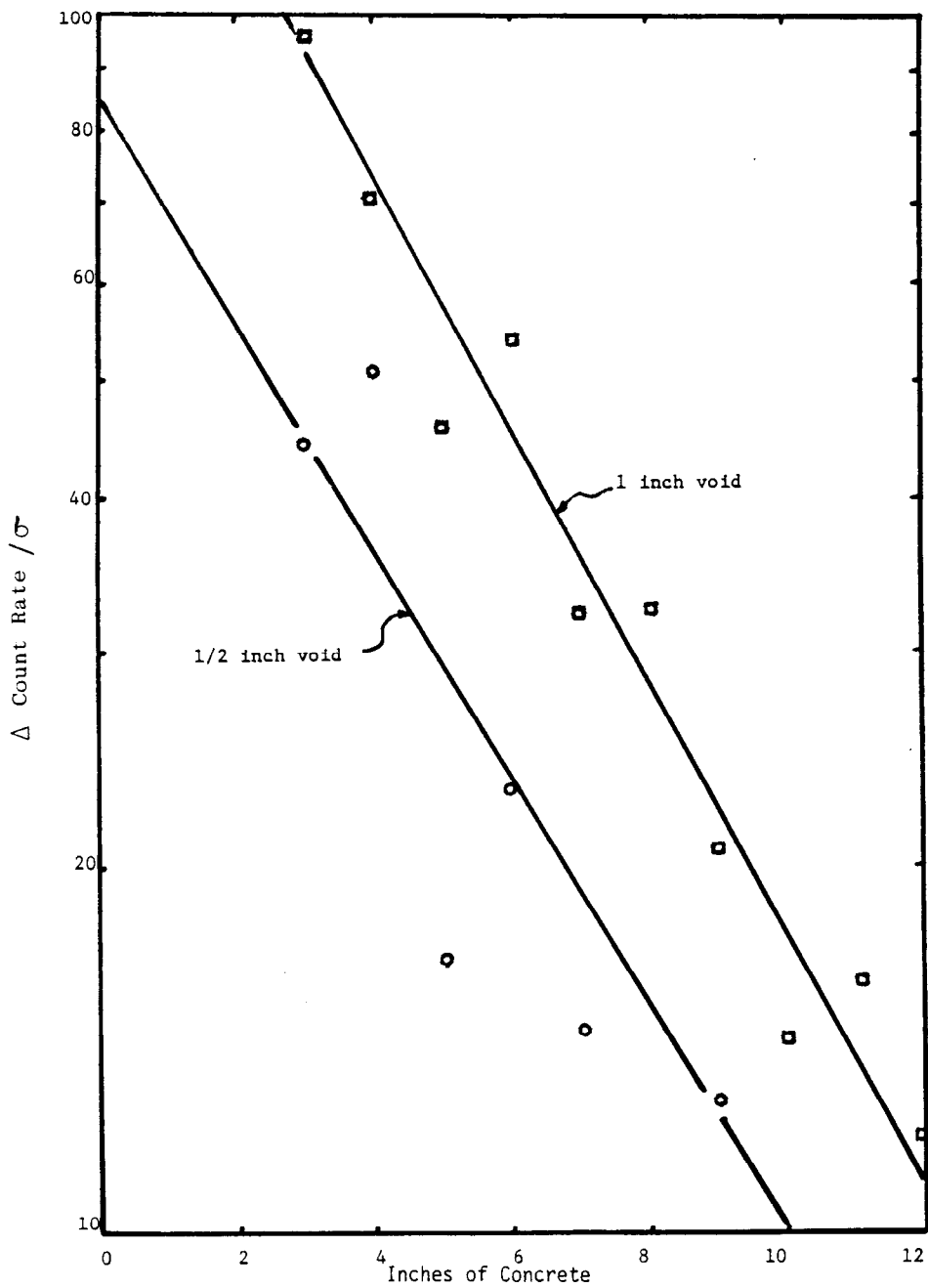


Figure 5-16

Ratio of Change in Count Rate to Standard Deviation for Count Rate vs. Transmission Path Lengths in Concrete

as the change in count rate exceeds the standard deviation for detection of the void, the void is detectable. By making longer measurements for the greater thicknesses or by averaging several readings, detection sensitivity is increased.

Backscatter

The choice of a proper gamma emitter is an important parameter in the design of a backscatter gage just as in the preceding section on transmission gages. The gamma emission must be below 1.02 MeV in energy to avoid pair production in the medium but above energies giving mostly photoelectric interactions. The isotope must have a long half life so that radioactive decay corrections will not have to enter into the daily calculations. Cesium-137 with a gamma of 0.66 MeV and half life of 30 years meets the above criteria.

The ease of operation will be important if the gage is to be used off the back of the slipform paving machine. The measurement must be able to be taken in a time period determined by the speed of the paving machine. The backscatter gage can make a measurement in a short period of time.

The gage used in this research operates effectively using a 5 to 10 microcurie (μCi) Cs-137 source. Radiological health and safety problems are negligible for this size source. Current regulations exempt Cs-137 sources of this size. Whole body exposure to the operator will be kept below the average exposure of 100 mr/week (5000 mr/yr radiation guide set by the Nuclear Regulatory Commission). The source is sealed in a plastic button which will eliminate the possibility of radioactive contamination. Although the source is small, the count rates obtained from it are large enough to give good counting statistics.

A single channel analyzer is used to electronically reduce the influence of the primary gamma at the detector. A lead shield, to separate the source and detector, also minimizes primary gamma interactions in the detector while maximizing the detection of Compton interactions in the concrete. These design considerations allow measurement of the density of the concrete. See figure 5-17.

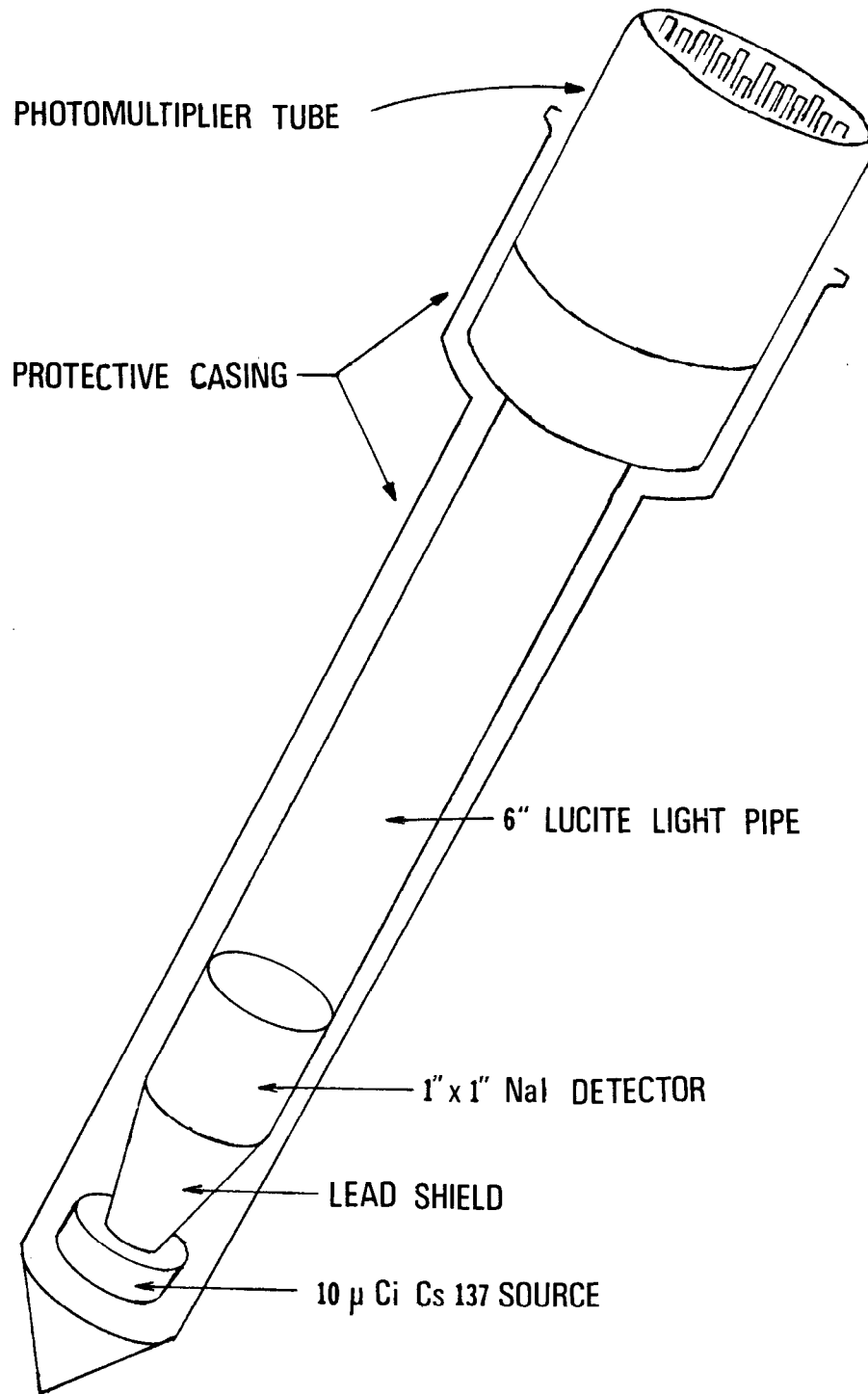


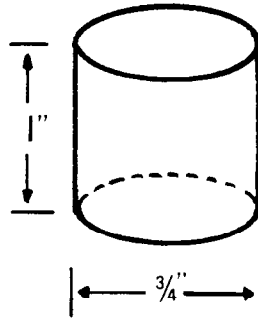
Figure 5-17
DIAGRAM OF BACKSCATTER GAGE

No previous work has been reported on a backscatter gage of this design, therefore much of the initial work was involved with the design. The critical part of the design was the geometry between the source and the detector. The source to detector distance (SDD) had to be kept small because of need for measurement of density in strata at selected vertical heights in the plastic concrete. If the SDD was large, a greater volume of material would be penetrated and the measurement would be an average of a large vertical thickness. An increase in the SDD would also decrease the gamma flux at the detector causing a decrease in the count rate. A factor which had to be balanced with the SDD was the amount of shield material between the source and the detector to reduce the effects of the primary gamma. Lead was chosen as the shield material because of its high density, availability, and workability.

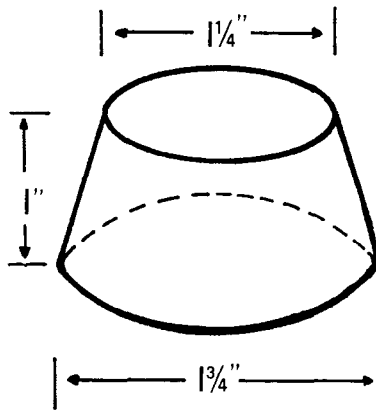
A 1 inch x 1 inch NaI crystal was chosen as the detector for the gage. It was chosen because of its size and efficiency in detecting gamma rays. The gage had to be less than 2 inches in diameter in order to fit in the calibration blocks used in this research and for ease of placement into a plastic concrete slab. There were two 2 inch diameter holes in each block, 12 inches apart. The blocks were 2 inches in depth, 22 inches in length, and 12 inches in width. The blocks were manufactured by the Louisiana Department of Transportation and Development to accommodate a Troxler Model 2376 transmission gage. The densities of the blocks were determined by their weight and volume. The blocks were also measured with a Troxler transmission density gage. This information is shown in Table 5-1. The blocks were radiographed to detect local anomalous density areas within the blocks. See figures 5-10 through 5-13 in the preceding section. Low or high density densities in the region around the holes have adverse effect on the calibration of the backscatter gage.

The first source-detector shield design, shown in figure 5-18, was a 1 inch cylinder 3/4 inch in diameter. The source's flux was measured with the source 1 inch from the crystal. With the shield

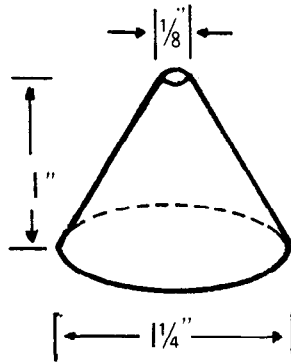
SHIELD 1
Cylindrical



SHIELD 2
Truncated Cone



SHIELD 3
Cone



* UNIT OF MEASURE : INCHES

Figure 5-18

SOURCE- DETECTOR SHIELD DESIGN FOR BACKSCATTER GAGE

in place between the source and the crystal, the count rate was reduced by a factor of 10.6. The gage was then tested in sample blocks of varying densities. A second shield was made in the shape of a truncated cone. Measurements were taken with it and compared to the cylinder. A third cone, 1 inch high and with a 1 1/4 inch diameter base, was fabricated. The three shields were compared and the results are shown in 5-19. The figure 5-19 contains 3 gamma ray spectra obtained with the various shield designs. The vertical axis is the counts per minute and the horizontal axis is the energy of the gamma ray. The 1 inch cone was determined to be the best design to maximize the count rate in the backscatter region for density measurements of thin vertical strata in the plastic concrete.

The signal to noise ratio was measured at increasing source to detector distances. The optimum source to detector distance was found to be 1 3/8 inches. See figure 5-20. The distance of 1 3/8 inches, however, did not give the maximum change in count rate between the high density blocks and the low density blocks. The best compromise between signal to noise ratio and the count rate difference was found to occur when the source to detector distance was 1 inch. See Table 5-2.

A light pipe was fabricated from a six inch lucite rod. The source, shield, 1 inch x 1 inch NaI crystal, lucite rod, and photomultiplier tube were assembled as shown in Figure 5-17. The rod provided a optical coupling between the NaI crystal and the photomultiplier tube. It also allowed measurements to be taken in samples up to eight inches in depth. The common thickness of a concrete highway slab is eight inches.

After the proper source to detector shield has been designed, measurements were made on the calibration concrete blocks. The blocks used had calculated densities of 135 pcf, 124 pcf, 116 pcf, and 99 pcf. Four 2 inches thick blocks were stacked on each other to model an 8 inch highway slab. The readings did **not** agree with the expected results.

GAMMA RAY SPECTRUM OF BACKSCATTER GAGE

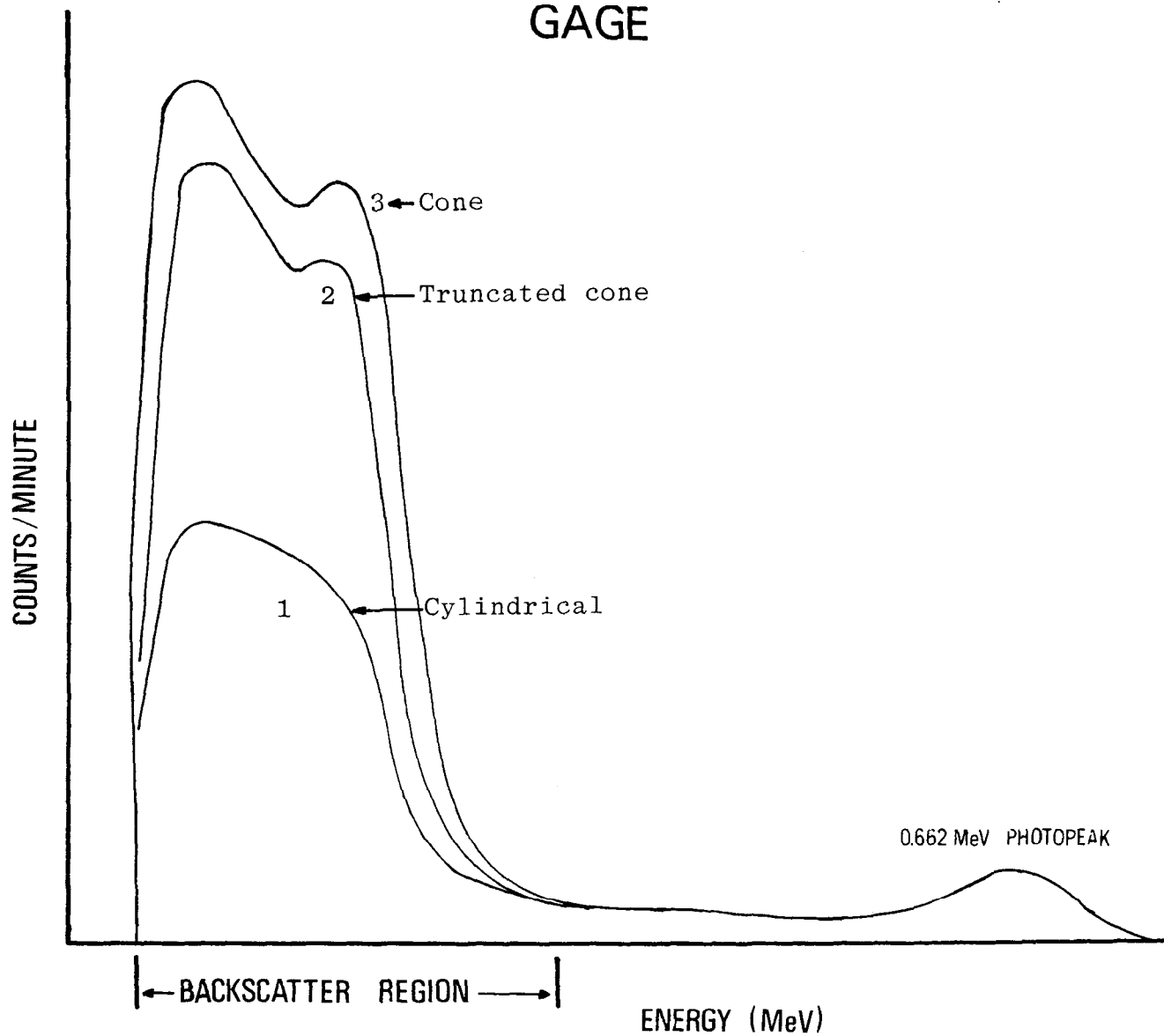


Figure 5-19

GAMMA RAY SPECTRA FOR BACKSCATTER GAGE; SOURCE-DETECTOR SHIELD DESIGNS

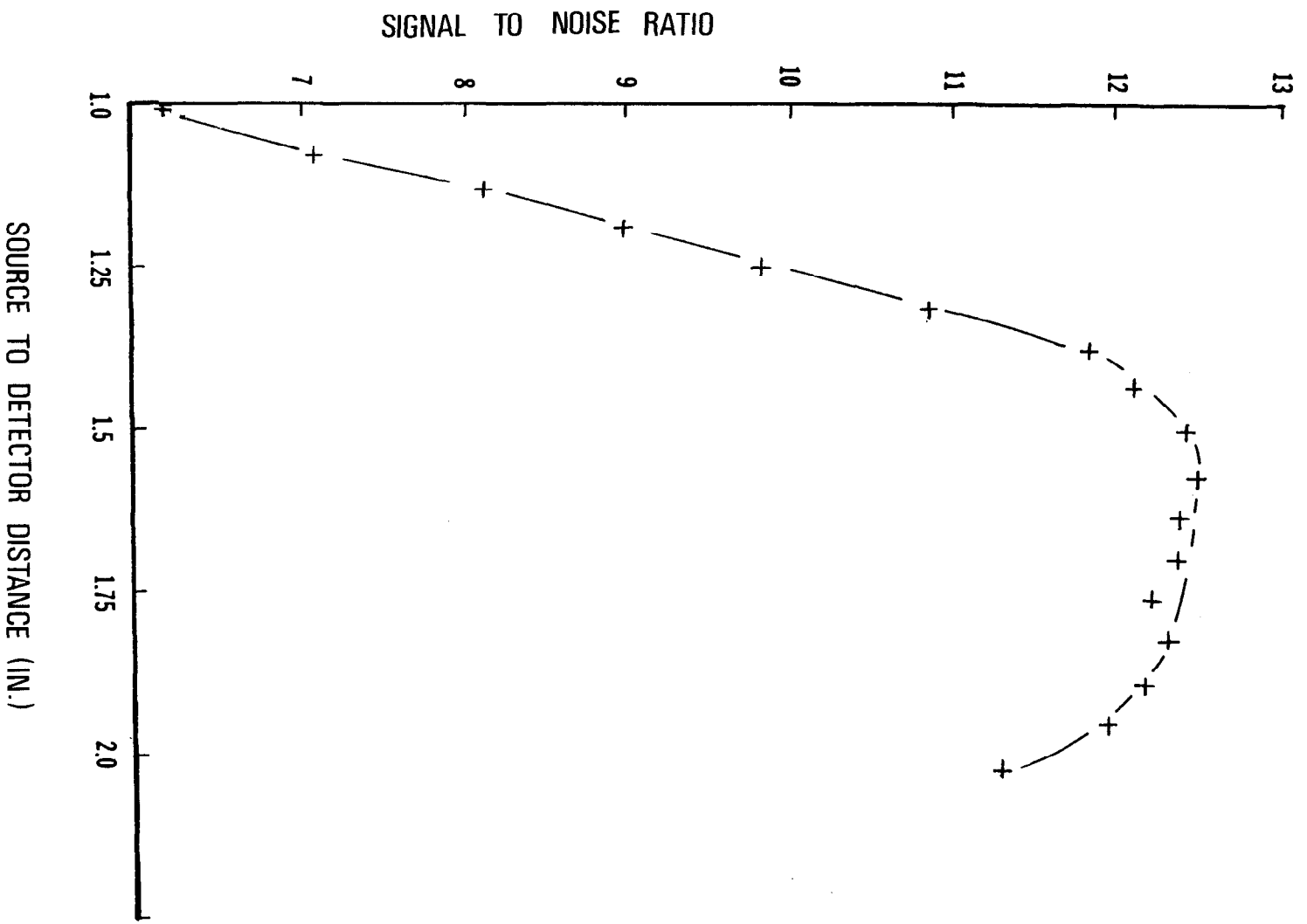


Figure 5-20

SIGNAL TO NOISE RATIO WITH INCREASING SOURCE TO DETECTOR DISTANCE

Table 5-2

Source to Detector Distance Optimization Data

In. Source-Detector	cpm		cpm air	Δ cpm	S/N
	low density	high density			
1	72740	91411	12201	18671	7.49
1 1/16	67503	82756	10307	15253	8.03
1 1/8	63415	78012	8865	14597	8.80
1 3/16	59230	72630	7589	13400	9.57
1 1/4	56227	69040	6892	12813	10.02
1 5/16	53914	65031	6331	11117	10.27
1 3/8	50683	62232	5752	11549	10.81
1 7/16	48783	59425	5574	10642	10.66
1 1/2	46922	56475	5316	9563	10.63

Low density - 99.3 lbs./ft.³

High density - 135.0 lbs./ft.³

However when compared to the densities determined by the Troxler transmission gage, the reading could be explained. The block densities, measured by the Troxler gage, varied from the density calculated from weight and volume measurements. The deviations resulted in a depression in the 125 pcf curves shown in Figure 5-21. The 125 pcf curve was depressed in the 4 to 5 inch region. The actual density of the 125 pcf curve in the 4 to 5 inch region was 122 pcf and the densities above and below it were 125 pcf and 126 pcf respectively. The 116 pcf curve depression was caused by a 13 pcf difference. The lower block was 107 pcf, while the one above it was 120 pcf. The backscatter gage measurements were then repeated using new blocks. These new curves were then compared to the original ones. This information was valuable because in one case a density difference of 3.6 pcf could be observed. The second set of curves is shown in figure 5-22.

In the next experiment a different density block was placed at various locations within the stack. The readings were taken and appear in figure 5-23. These results showed that the backscatter gage could be used to determine the density of the concrete at a different strata. This experiment shows that the gage reasonably satisfied the need to measure strata in a concrete slab.

Calibration curves were made for each depth as shown in figure 5-24.

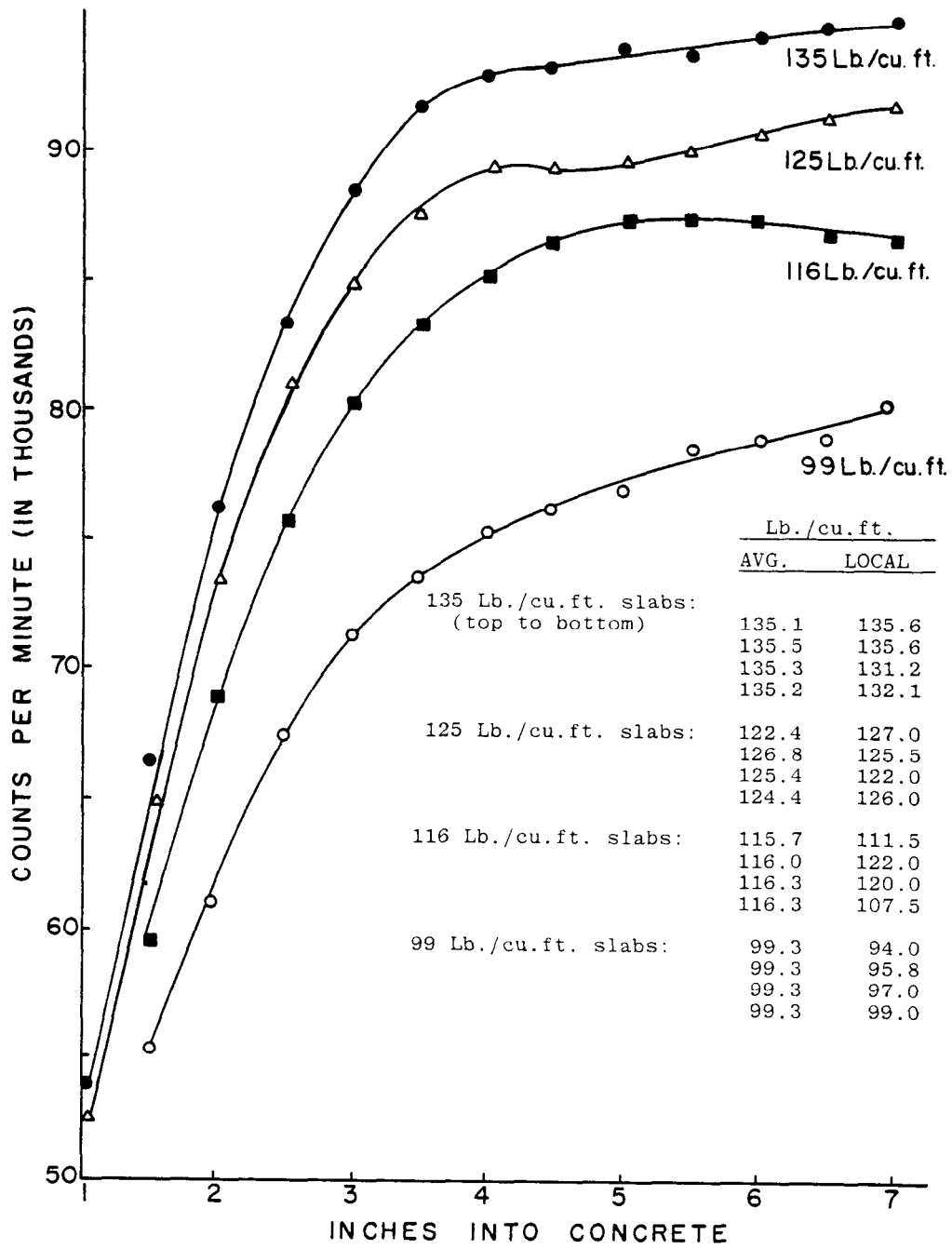


Figure 5-21
BACKSCATTER GAGE MEASUREMENTS ON STANDARD SLABS

DENSITY CURVES

UNIFORM DENSITY BLOCKS

DENSITY DETERMINED BY WEIGHT AND VOLUME RELATIONSHIP

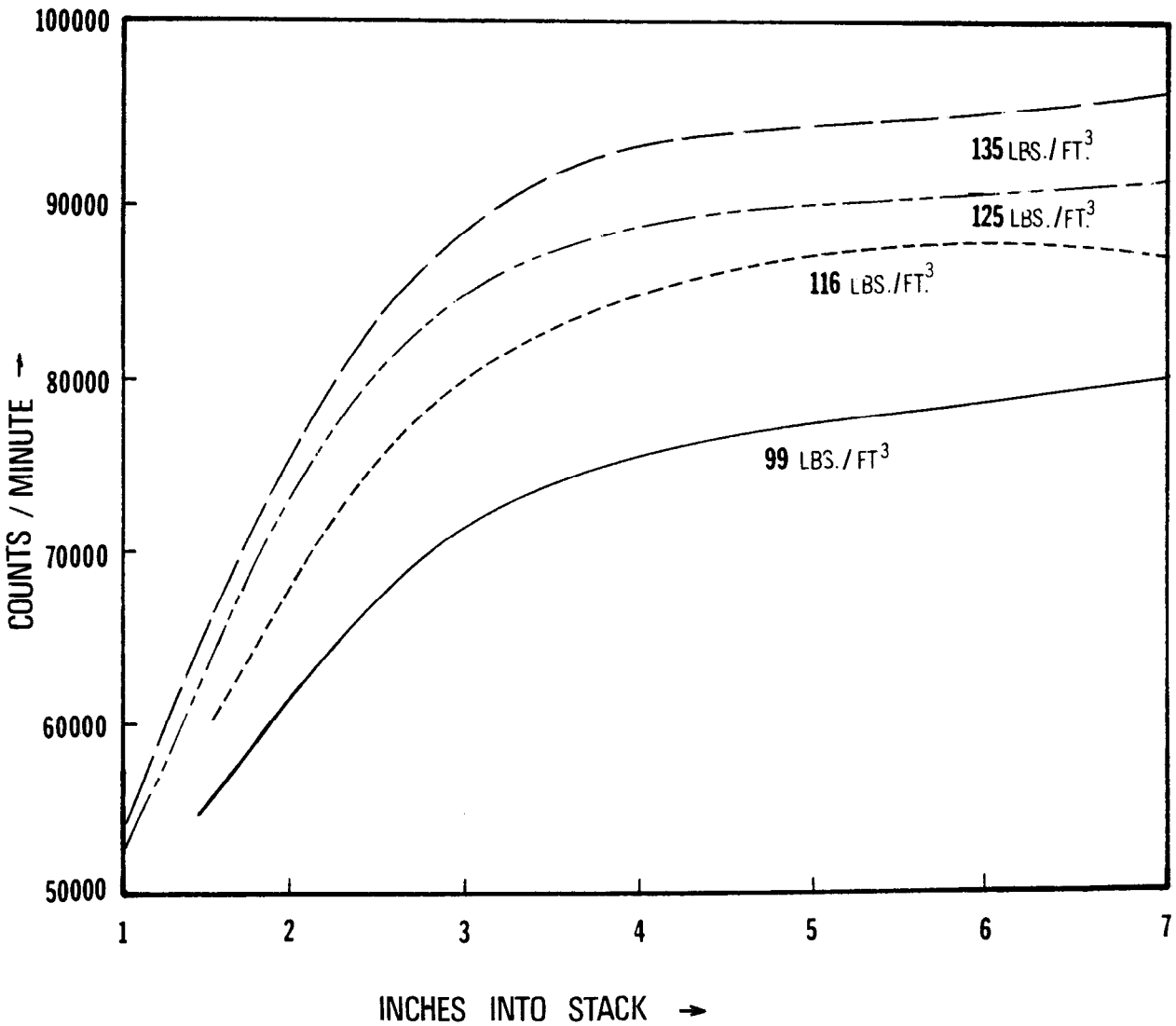


Figure 5-22

BACKSCATTER GAGE MEASUREMENTS ON UNIFORM STANDARD SLABS

DENSITY CURVES

A 99 LBS./FT.³ BLOCK WAS PLACED IN VARIOUS POSITIONS
IN A STACK OF 134 LBS./FT.³ BLOCKS

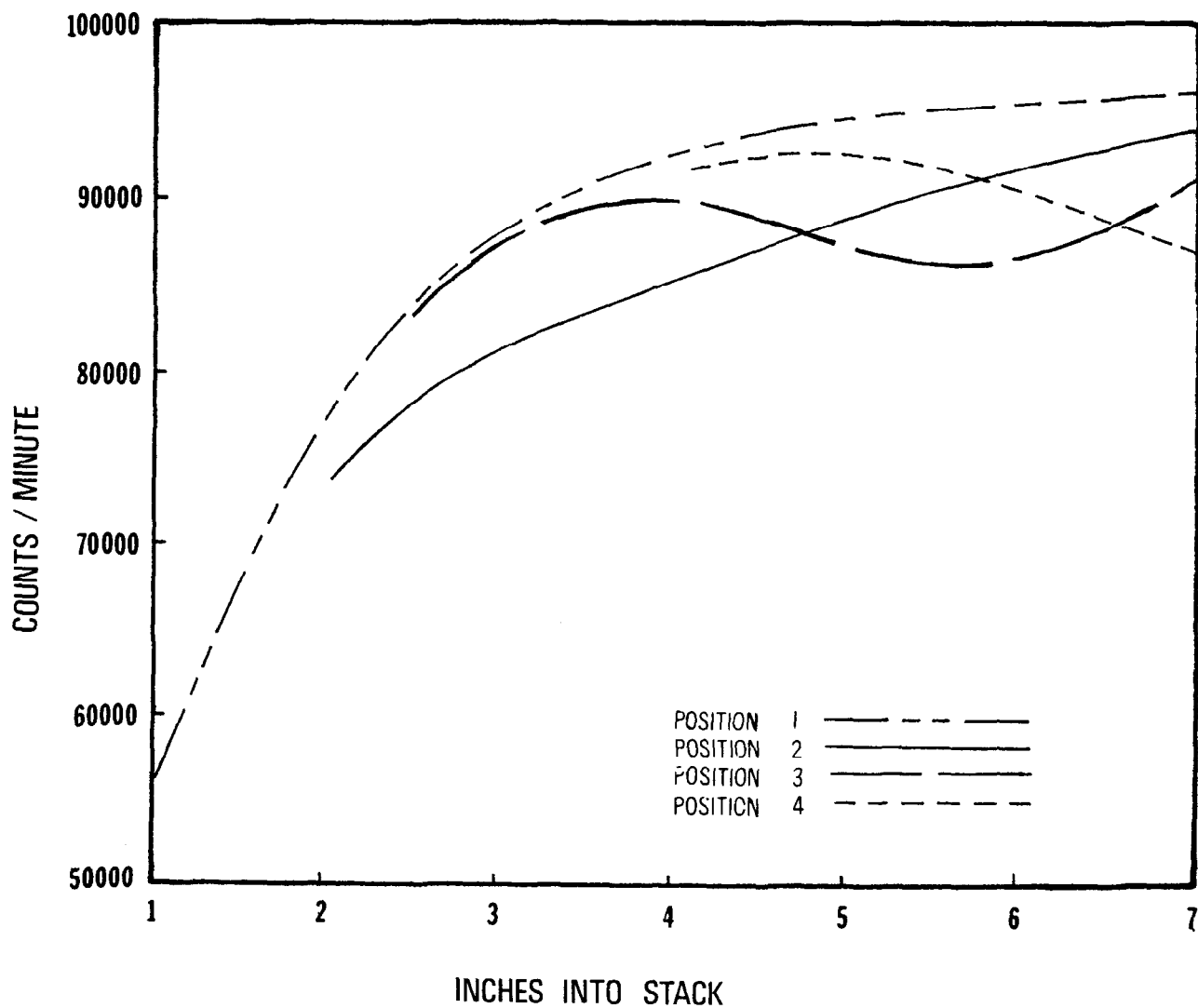


Figure 5-23

BACKSCATTER GAGE MEASUREMENTS ON NON-UNIFORM STACKS OF STANDARD SLABS

CONCRETE CALIBRATION CURVE

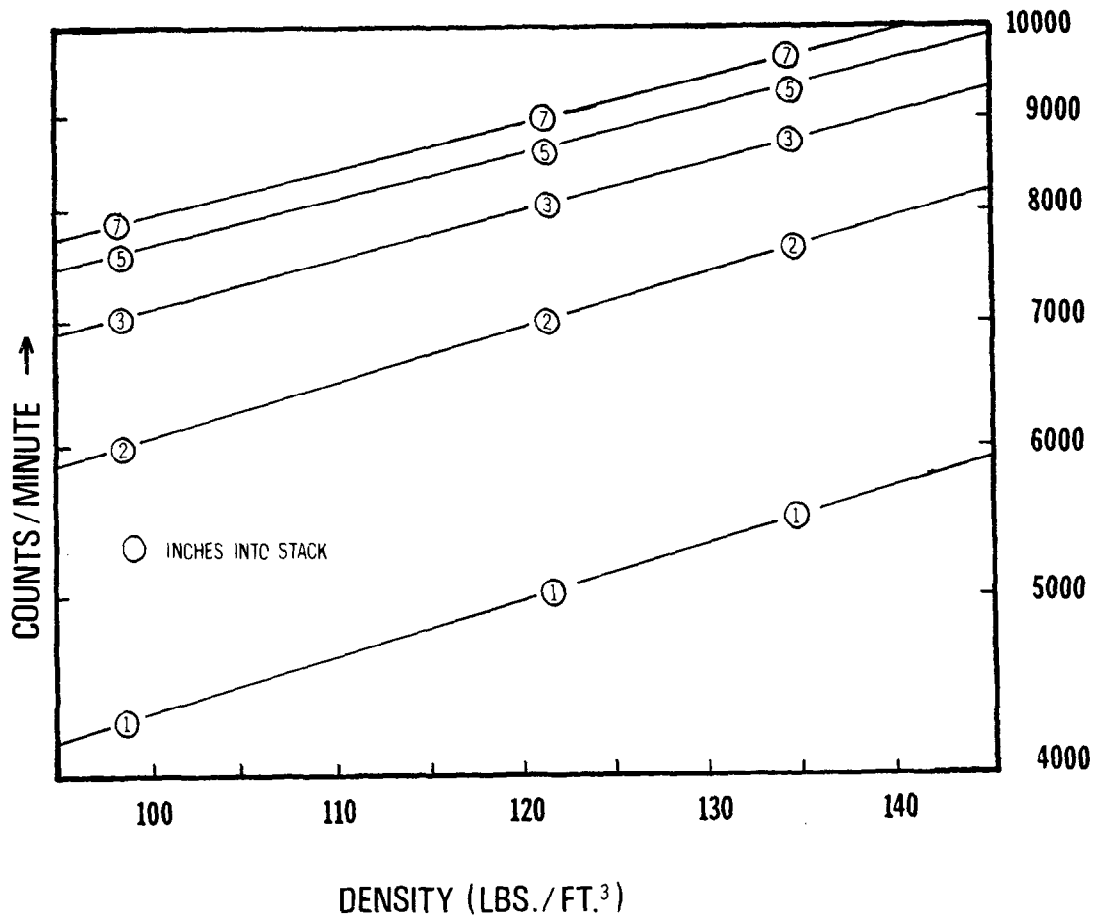


Figure 5-24

CONCRETE CALIBRATION CURVES WITH DEPTH

CHAPTER 6

FIELD DENSITY RESULTS

Density of plastic concrete in the field was determined on seven construction projects using the Troxler Model 2376 dual probe transmission gage. The source detector system used for the field work is shown in Figure 5-8 and 5-9. Measurements were taken in regular concrete pavements (Proj. A-D), bridge approach slab (Proj. E), and bridge deck slabs (Proj. F & G). Results obtained on each project are listed in Appendix B.

Discussion of Results

Test sites were selected either near the pavement edge or from an equipment bridge at the rear of the paving machine proper, as conditions allowed. Calibration readings were taken prior to and after each set of readings as a check on equipment function and to determine the standard count. The density values for each site were determined using tables provided by the manufacture. No problems were encountered in use of the nuclear equipment.

The readings were obtained at each site after the source detector system was manually pushed, vertically, into the plastic concrete and the cone shaped tips were in contact with the underlying material. Readings were taken at a known depth relative to the surface of the concrete. The depths of each test on the tables listed in appendix B indicates the distance of the source and detector below the surface on top of the concrete. The effective vertical extent of density measurement is considered to be a 1 inch thick horizontal layer. Between the source and the center of the detection crystal. This range is not constant for the 12 inches, but is variable depending on proximity to the source or detection crystal. Readings were taken at two inch increments of depth below the first level of test, and in some cases every inch. While the measurements taken every inch overlap,

they were taken to determine the vertical influence of steel reinforcement.

Pushing the source detector system in low slump concrete used in slip-form paving was a problem on one project. This was rectified by modifying the conic probe tips to a sharper point. Additional work needs to be done to determine if placement of the system can be automated. Possibly the gage could be attached to some part of the paving train and hydraulically push the probes into the plastic concrete.

Steel reinforcement in bridge decks did not present a serious problem in placement of the system. It does help, however, to know the rebar lay-out before hand. Nuclear readings were affected in some cases; however, when this did occur it was very evident, and thus, could be discounted in vertical series of readings.

The nuclear readings indicated low and non-uniform density values on one project--Project B. Although non-uniform vertical values were obtained on other projects, this project had much greater variation. Tests were taken during a period when problems developed at the batch plant. The plant was producing very dry and very wet batches. Honey comb structure could be expected from the very dry batches and was reflected by low and non-uniform density values. Cores verified the honey comb structure. The cores at low density sites, but not showing large voids, probably represent areas of wet batches.

Overall there was no major problem in using the nuclear device for determining densities in a horizontal layer. The instrument did show density resulting from honey comb structure or high slump concrete, both of the conditions are normally not acceptable.

CHAPTER 7

LABORATORY TESTS ON EFFECTS OF REINFORCED STEEL

In the discussions of field density results (Chapter 6), it was indicated that nuclear readings taken in bridge decks were affected by the steel reinforcement in some cases. The readings that were affected in a vertical series were easily recognized and discounted. The density measurements one inch above/or below the effected levels of measurements appear to be valid density values for the concrete mass in each case. (See tables 6B through 9B, inclusive, in Appendix).

In order to obtain additional data as to the effect of steel on the nuclear readings, tests were conducted on laboratory models containing different sizes and arrangements of steel rebars. Steel rebars were placed in a wooden box containing dry siliceous coarse-graded sand between aluminum access source/detector tubes. The sand placed in each model was not compacted in order to have as much density differential between steel and sand as possible. The dimensions of the wooden box were 15 by 25 by 24 inches in height. The box and two different test models are shown in figures 7-1, 7-2 and 7-3. Figure 7-4 illustrates a typical steel rebar layout encountered on a bridge deck tested. Two sizes of steel rebars were used in the laboratory model tests; number 5 (0.625 inch diameter) and number 10 (1.27 inch diameter).

Plots of nuclear densities determined by taking a series of vertical nuclear readings (at one-tenth of an inch increments) in two models are shown in figures 7-5 and 7-6. The readings were taken through two layers of steel rebars separated by sand, with one rebar (figure 7-5) and three rebars (figure 7-6) in each layer between the source and detector.

Figure 7-7 and 7-8 are similar plots as described above with a single number 10 rebar between source and detector. In one case (figure 7-7), the rebar is centered between source and detector, and in the other

(figure 7-8) a dual plot with rebar near source and then near detector. The nuclear readings were taken in increments of 0.25 inches in these tests.

The results of these tests, as shown in the figures, also appear to substantiate the validity of density values obtained one inch above or below steel reinforcement rebars as discussed earlier, regardless of the rebar size (normally used in bridge decks) or position (relative to source or detector). The influence of steel reinforcement on nuclear readings should not be a major problem when using this technique since low density values are of primary concern and any effect from steel rebars should result in a density equal to or above that for the concrete mass itself. It is recommended, therefore, that only nuclear readings obtained outside of a one inch zone from any steel rebars be used in evaluating the consolidation of concrete. Any nuclear densities obtained within this zone should be considered affected by the rebars and discounted. It would be helpful toward this end in knowing the approximate location of steel reinforcement beforehand.

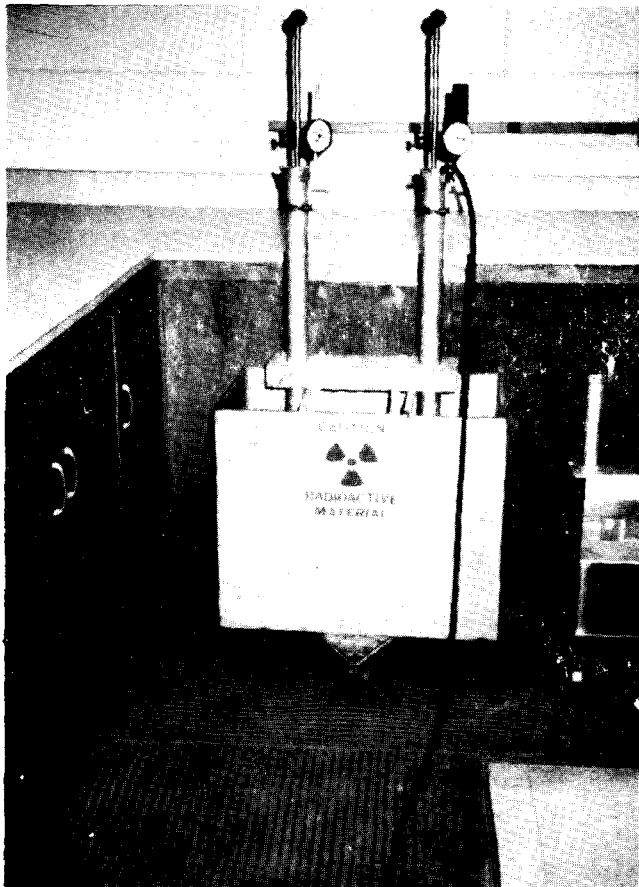


Figure 7-1: The box and source/detector tube setup for laboratory tests of models.



Figure 7-2: A test model with two rebars between source/detector access tubes.

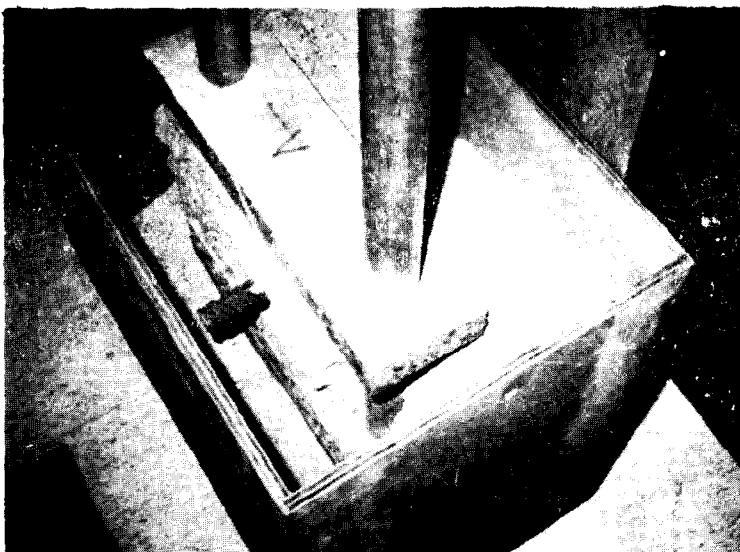


Figure 7-3: A test model with a single rebar centered between source/detector access tubes.

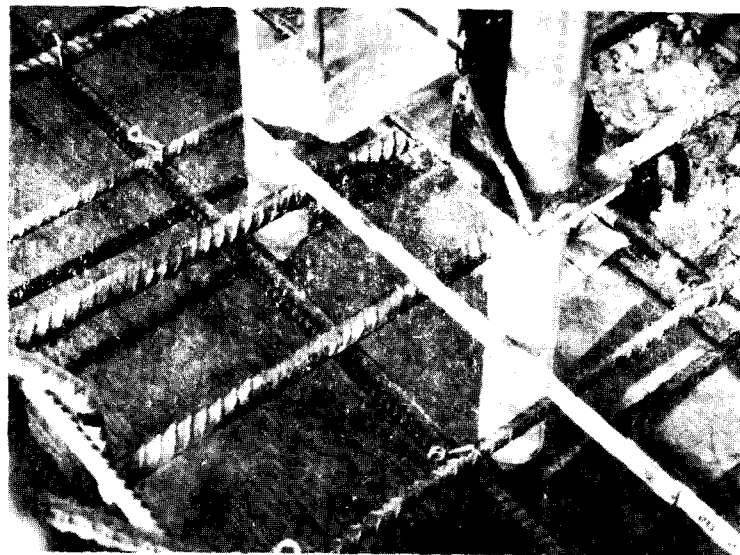


Figure 7-4: A typical steel rebar layout encountered on a bridge deck tested.

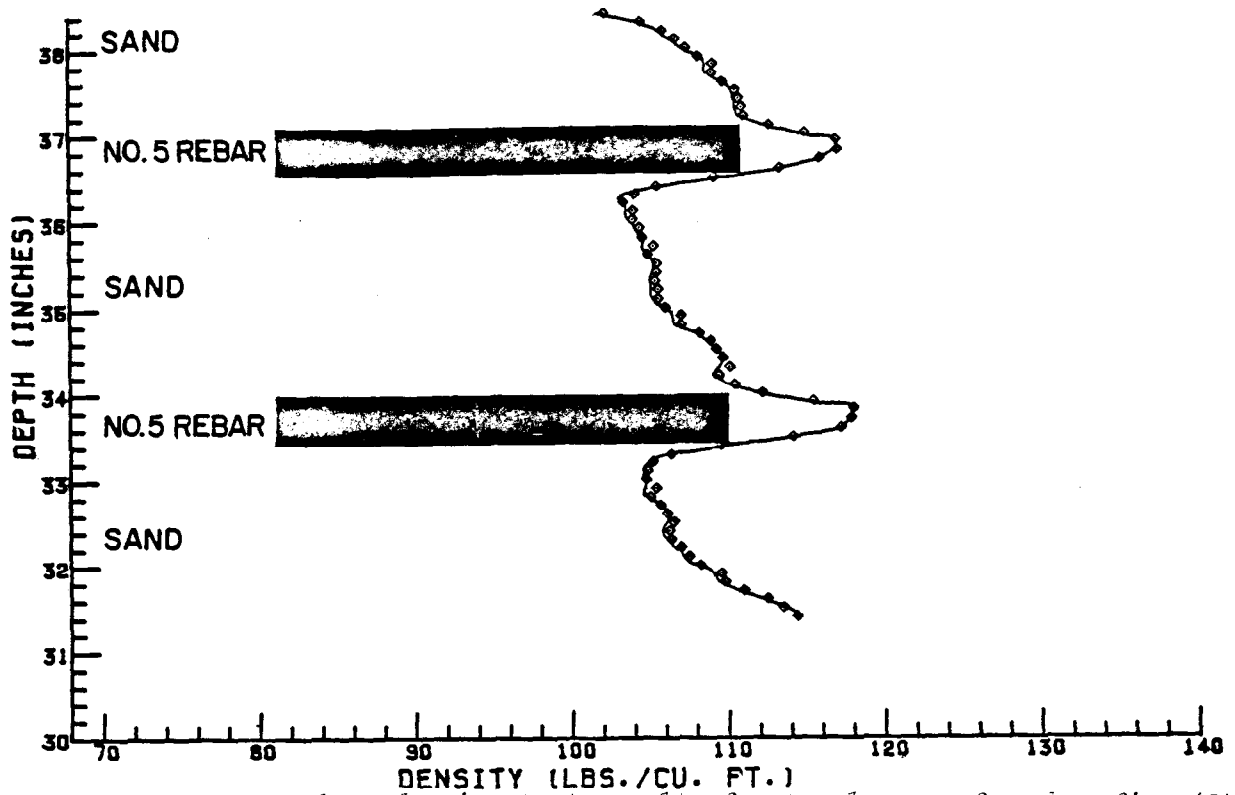


Figure 7-5 Plot of nuclear density test results for two layers of number five (5) rebars with one (1) bar in each layer between source and detector.

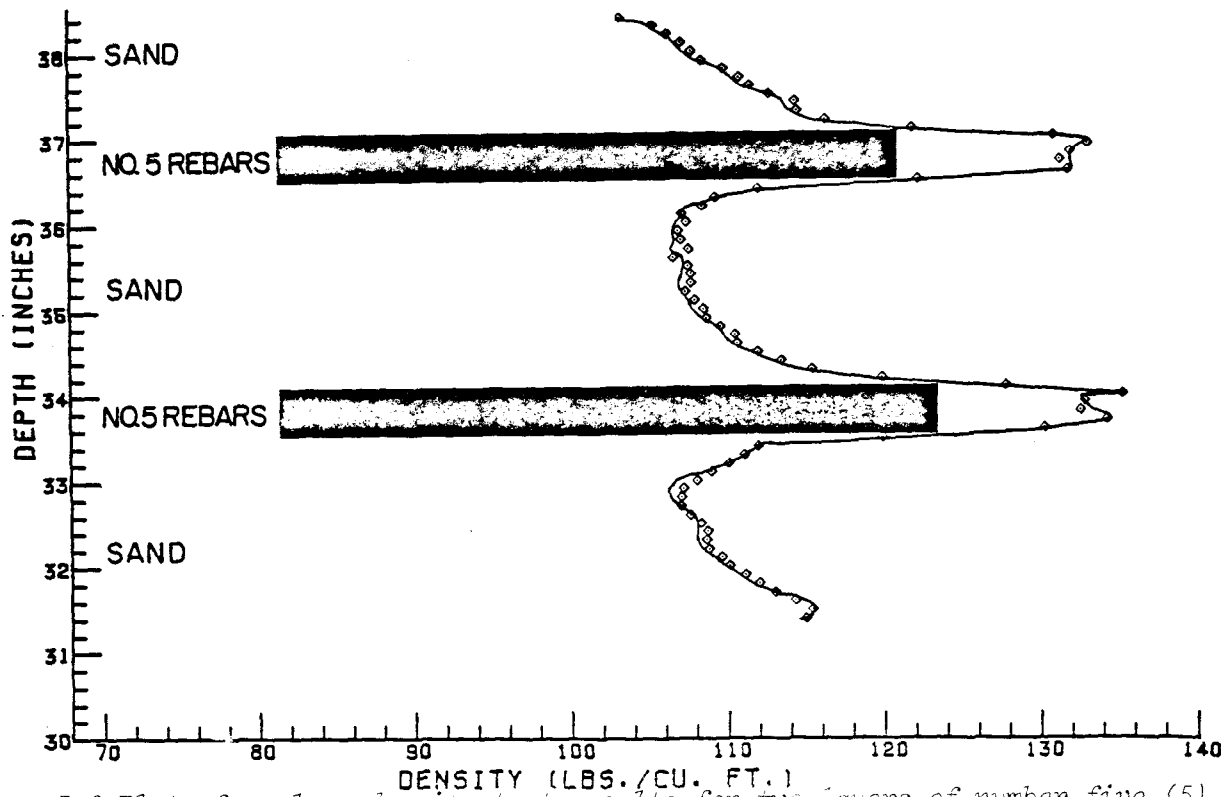


Figure 7-6 Plot of nuclear density test results for two layers of number five (5) rebars with three (3) bars in each layer between source and detector.

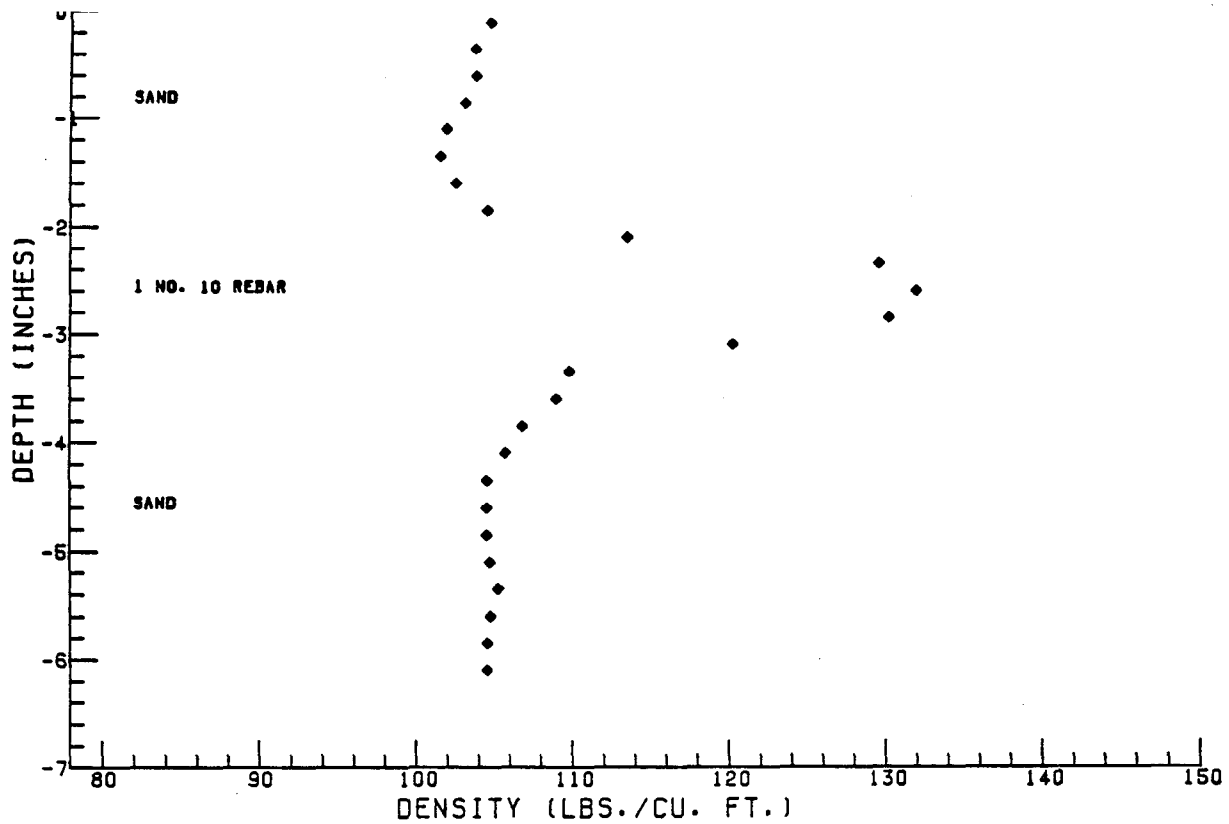


Figure 7-7 Plot of nuclear density test results for lab model with one (1) number 10 rebar centered between source and detector.

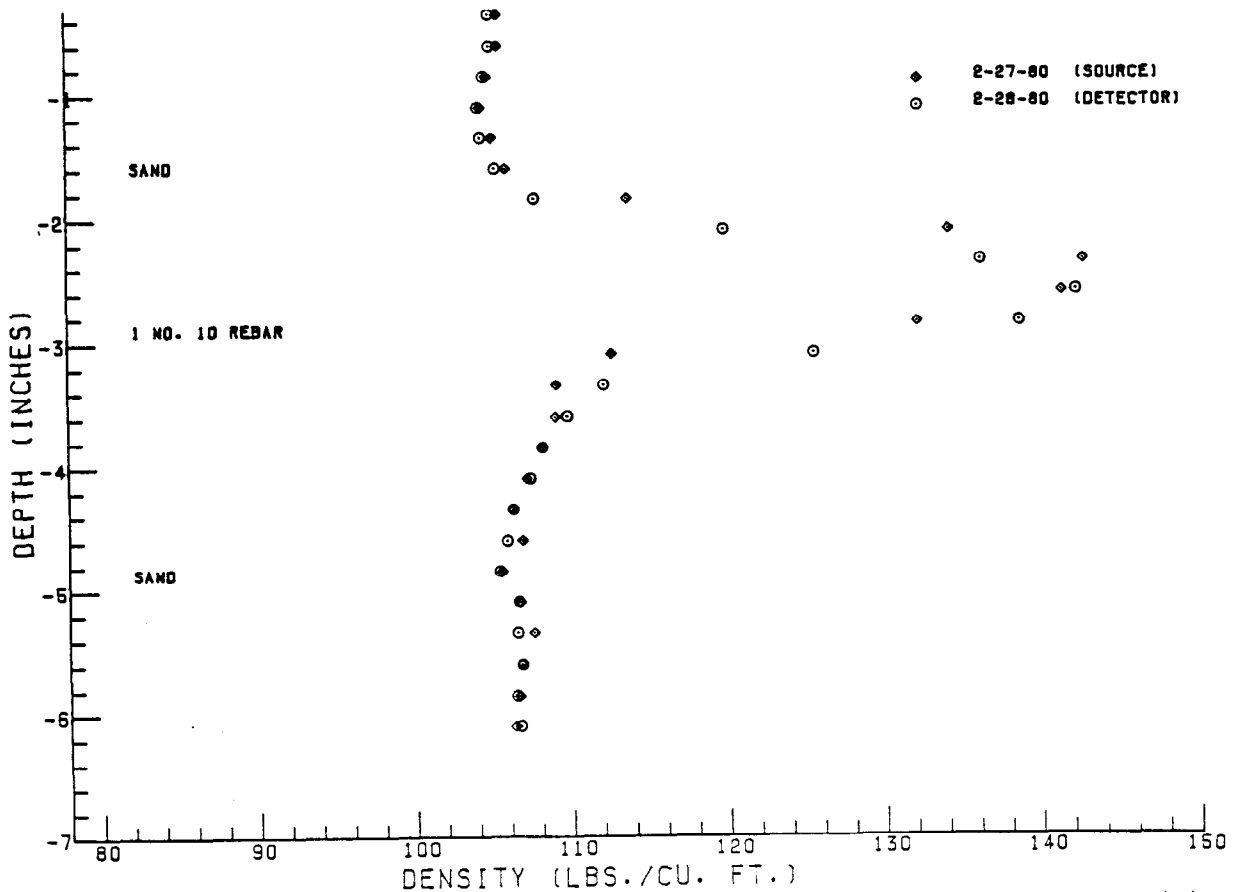


Figure 7-8 Plot of two sets of nuclear density tests results with one (1) number 10 rebar, rebar placed near the source in one set of nuclear readings and near the detector in the other.

CHAPTER 8

CONCLUSIONS

The comparison of transmission and backscatter gages for measurement of concrete density in vertical strata shows each to have advantages and disadvantages.

Based on the listing of advantages and disadvantages in Table 8-1 and on field experience with the equipment, the Troxler Model 2376 dual probe transmission gage functions best and provides the most reliable results. The gage using a source in a tube under the roadway and a detector scanning horizontally across the roadway above that tube is not available commercially and would be difficult to handle and set up in the field. The single probe backscatter gage demonstrated poor stability and considerable difficulty in calibration (each strata measured has a different calibration curve as the result of bottom and top effects). The backscatter gages offer poorly defined sample localizations. The surface backscatter gage (Troxler 3400) also only provides density information for the surface backscatter gage (Troxler 3400) only provides density information for the surface layers, no information is obtained from the bottom layer. Surface backscatter is however, a stable, easily read, available technique and far better than no measurement at all.

The Troxler Model 2376 could be improved by decreasing the size of the hole punched by the source tube. Presently both the source and detector tubes are 2 inches in diameter. The source tube could easily be 1/2 inch in diameter without losing any of the present design advantages. A 1/2 inch diameter source tube is possible but may prove to be insufficiently rigid to provide the reproducible source to detector spacing required.

A decrease in the diameter of the detector would also ease insertion

of the detector tube into the concrete. However, a decrease in the size of the detector would also decrease sensitivity and increase counting time. Smaller scintillation detectors may also suffer from poorer stability.

By putting a source in the third leg of the modified probe, an increase in sample volume inspected would be obtained but sensitivity for voids would be decreased. Improvement in the probe tips to permit inspection of the bottom layer is desirable, but probably impractical. It should be possible to push hollow tubes into the plastic concrete, auger out the concrete in the tubes and place the detector and source at the very bottom layer. Whether this procedure would be worthwhile depends upon the value of detecting voids in the very bottom layer of the slab.

Table 8-1

Concrete Density Gaging Techniques with their
Advantages and Disadvantages

<u>Technique</u>	<u>Advantages</u>	<u>Disadvantages</u>
Transmission Vertical scan (Troxler Model 2376)	High sensitivity Good vertical localization of voids Commercially available, simple modification Rugged and dependable Easily calibrated Good calibration curve Easy to operate Good stability	Must make 2 holes in slab Small volume inspected Cannot measure to bottom of slab Somewhat clumsy Large disturbance of sample Slower than backscatter Moderate size radioactive source (5 mCi)
Transmission Horizontal scan	High sensitivity Good horizontal location of voids Large sample inspected Does not disturb voids Can give a record (strip chart) Easy to operate, automatic Indicated rebar placement Easy, stable calibration No holes in slab, no repair	Requires source to detector distance control No vertical localization Cannot sample after the fact-must plan inspection points in advance No commercial supplies Difficult to set up May be very difficult to do on slabs poured adjacent to another slab Moderate sized source (5-10 mCi)
Backscatter Vertical probe	Single probe, single hole Very fast (<1 minute) Small source (5-10 μ Ci)	Small sample volume measured Much of sample disturbed

55

(Continued)

Technique

Advantages

Disadvantages

	Very compact	Hard to calibrate
	Simple and safe to operate	Poor stability
		Large top and bottom effects
Backscatter	Commercially available	Only measures surface
	Normally already on hand	No vertical localization
Surface Measure-	Easy to operate	Sensitivity decreases with
ment	Very stable	depth
(Troxler 3400 or	Good Calibration	Moderate source (8mCi) plus
equal)	Can be used for other meas-	neutron source
	urements	

RECOMMENDATIONS

The intent of this research effort was to determine the feasibility of using a nuclear technique to determine the density of thin layers of plastic concrete. This was accomplished along with the determination that a dual probe gage used in the research, was practical for this use after minor modification of its source-detector tubes. The unit used in this study had 2 inch diameter tubes and one or both could possibly be less without the loss of any design advantages and with less effort required to push the unit into the plastic concrete. Additional research is recommended to reduce the diameter of both the source and detector tubes.

It is recommended that the dual probe technique be considered for field application by the Department in a job control mode. Use of this technique would provide a rapid evaluation of the uniformity and level of consolidation of plastic concrete achieved by the Contractor's placement and vibration effort in pavement or bridge deck construction. Data would be available at a very early stage of construction indicating good consolidation or the need to make corrections in subsequent operations.

Obtaining suitable data points for evaluation will require that a proper sampling scheme be established. Density values of plastic concrete should be taken on several projects, prior to full field application, in order to develop lot size, number of samples per lot and depth or depths to be checked within the concrete pavement or bridge deck. Any individual test should be taken at least 1.25 inches below the concrete surface and a minimum of 1.0 inch above or below any steel reinforcement bars whenever the test site is in reinforced concrete pavement or bridge deck.

Establishing a minimum level of consolidation (density) of plastic concrete needed to assure performance or durability of the hardened concrete during the design life of the pavement or bridge deck was

beyond the scope of this research effort. A literature search and discussion with numerous persons knowledgeable in concrete did not reveal enough information for the authors to recommend a specific unit weight or percentage of a standard for the Department to use as minimum acceptance criteria. Colorado is the only State currently with a nuclear gage based specification for pavements to our knowledge. The State uses direct transmission measurements to enforce a requirement that the concrete be vibrated to not less than 96 percent of the maximum theoretical field density. This percentage was established from a research study entitled, "The Effect of Vibration on the Durability of Unreinforced Concrete Pavement," which showed that cores from pavements with poor abrasion records had densities less than 97 percent of rodded unit weight. It is therefore recommended that research be conducted in order to develop a minimum degree of consolidation (density) of plastic concrete that could be used as acceptance criteria. Until such time as an acceptable minimum value is determined by research, it is recommended that 96 percent of a standard unit weight be used experimentally as a minimum target above which consolidation is considered proper. This standard unit weight should be determined for each lot in the field using test method LA DOTD TR: 201-77.

APPENDICES

APPENDIX A

Core Scanning Equipment, Procedures, and Results

Core samples taken after field studies on paving projects needed to be evaluated for comparison of results. These cores were examined by both manual and automatic radiation density measurements. Both procedures used a Cs-137 gamma source and a NaI(Tl) detector for density measurements in the transmission mode.

Manual

The Troxler Model 2376 electronics package and detector were used with two 5 μ Ci Cs-137 laboratory check sources (10 μ Ci total activity). The sources and detector were collimated to provide a narrow inspection beam passing through the diameter of the core samples as shown in Figure A-1.

After tuning the Troxler gage detector with the sources and detector at the middle of the core sample 44 + 25, each core was scanned down its length, taking one minute counts at 1 inch intervals along the vertical axis of the core. Then a one minute count was made with nothing but air between the source and detector. Next, 4 inches of aluminum absorber was placed between the source and the detector and a 1 minute count was made. Aluminum was chosen as the standard because it has a density very close to concrete as far as gamma rays are concerned. Having the count rate with no absorber (I_0), a count rate with 4 inches of aluminum (I), the density and thickness of the aluminum, a mass absorption coefficient was calculated from

$I = I_0 e^{-\mu_m \rho t}$. Using the calculated mass attenuation coefficient and the counts per minute detected, within the Cs-137 peak, passing through the core sample as the I count rate, densities for each 1 inch interval of the core sample were calculated. The data collected and the corresponding density values for each core sample are listed in Table A-1. The densities calculated for the core samples calculated using the scanner data compared to the densities obtained using the Troxler gage were rather high, with differences of 5.0 to 14.8 percent. The large difference was probably due to the fact that the geometries of the aluminum standard and the core samples were not the same. The cores were cylindrical and the aluminum standard was rectangular. This means that the entire surface area of the detector had 4 inches of aluminum between it and the Cs-137 sources while only a small portion of the detector's surface area had 4" of concrete core (the diameter of a circle) between detector and the sources. This would cause the mass attenuation coefficient of the standard to be different from that of the core samples and results in a significant difference between the core samples densities and the "in field" highway densities measured with the Troxler gage. Because of the large density differences mass attenuation coefficient was recalculated using the core sample 43 + 75 as the standard. The reason for choosing the 43 + 75 core sample as the standard was because it had the most constant count rate over its length. The standard density used for the core was taken as the average of the 7 densities measurements made of the concrete highway slab at road marker 43 + 75 with the Troxler gage. The average density was 138.3 PCF or 2.215 g/cm^3 . The (I) count rate used for the core was the average of several 1 inch interval counts made with the scanner. Using the average density, the average counts/min of the core and the previously obtained I_0

count rate mass attenuation coefficient was recalculated. Then using the new mass attenuation coefficient, the counts per minute passing through the core, the I_0 count rate, new density values were calculated for both core samples 44 + 25 and 44 + 100. These results can be found in Table A-2. As can be seen from this data, the % difference in the density measurements made of the poured concrete and the densities of the core samples was much less than those obtained previously using the aluminum standard, i.e., differences range from 0.06 to 4.4 percent. This resulted in a difference in density no larger than 6.0 pcf.

TABLE A-1

CORE SAMPLE DATA USING ALUMINUM STANDARD

I_0 (no absorber) = 5794.3 c/m
 I (standard = 4" of Al) = 1159.8 c/m
 ρ (density of Al) = 2.699 g/cm³
 μ_m (mass absorption coefficient) = 0.596 cm²/g
 t = 10 cm
 conversion factor = 62.43 pcf./g/cm³

Core Sample 44 + 25

inches down core	counts/ min	average core density from manual scan	corresponding field measured density	% difference in density
1	1347.0	152.8 pcf.	(no data)	
2	1319.0	155.0 pcf.	" "	
3	1358.5	151.3 pcf.	" "	
4	1347.0	152.8 pcf.	143.2 pcf. at 4 1/2" in- to hwy slab	6.7%
5	1301.7	156.4 pcf.	143.2 pcf.	9.2%
6	1274.0	158.7 pcf.	142.7 pcf. at 6 1/2" in- to hwy slab	11.2%
7	1315.5	155.3 pcf.	142.7 pcf.	8.9%

Rotated Core 44 + 25 by 90°

1	1343.0	153.1 pcf.	(no data)	
2	1302.3	156.4 pcf.	" "	
3	1307.3	156.0 pcf.	" "	
4	1368.5	151.2 pcf.	143.2 pcf. at 4 1/2" in- to hwy slab	5.6%
5	1247.5	160.7 pcf.	143.2 pcf.	12.2%
6	1244.0	161.2 pcf.	142.7 pcf. at 6 1/2" in- to hwy slab	13.0%
7	1379.0	150.4 pcf.	142.7 pcf.	5.4%

TABLE A-1 Con't.

Core Sample 44 + 100				
inches down core	counts/ min	average core density from manual scan	corresponding field measured density	% difference in density
1	1457.5	144.6 pcf.	(no data)	
2	1373.5	150.8 pcf.	138.6 pcf. at 2 1/2" in- to hwy slab	8.8%
3	1333.0	153.9 pcf.	138.6 pcf.	11.0%
4	1255.5	160.2 pcf.	142.6 pcf. at 4 1/2" in- to hwy slab	12.4%
5	1266.0	159.3 pcf.	142.6 pcf.	11.8%
6	1358.0	152.0 pcf.	140.0 pcf. at 6 1/2" in- to hwy slab	8.6%
7	1339.0	153.5 pcf.	140.0 pcf.	9.6%
Rotated Core 44 + 100 by 90°				
1	1407.0	148.3 pcf.	(no data)	
2	1392.5	149.3 pcf.	138.6 pcf. at 2 1/2" in- to hwy slab	7.7%
3	1285.0	157.8 pcf.	138.6 pcf. a	
4	1252.0	160.5 pcf.	142.6 pcf. at 4 1/2" in- to hwy slab	13.9%
5	1370.5	151.0 pcf.	142.6 pcf.	5.9%
6	1348.5	152.7 pcf.	140.0 pcf. at 6 1/2" in- to hwy slab	9.1%
7	1249.0	160.7 pcf.	140.0 pcf.	14.8%

TABLE A-1 Con't.

Core Sample 43 + 75				
inches down core	counts/min	average core density from manual scan	corresponding field measured density	% difference in density
1	1349.0	152.7 pcf.	(no data)	
2	1342.5	153.2 pcf.	138.6 pcf. at 2 1/2" in- to hwy slab	10.5%
3	1328.5	154.3 pcf.	138.6 pcf.	11.3%
4	1338.5	153.5 pcf.	139.5 pcf. at 4 1/2" in- to hwy slab	10.0%
5	1305.3	156.1 pcf.	139.5 pcf.	11.9%
6	1355.3	151.3 pcf.	136.5 pcf. at 6 1/2" in- to hwy slab	10.8%
7	1335.7	153.7 pcf.	136.5 pcf.	12.6%
Rotated Core 43 + 75 by 90°				
1	1337.3	153.6 pcf.	(no data)	
2	1424.5	147.0 pcf.	138.6 pcf. at 2 1/2" in- to hwy slab	6.1%
3	1275.3	158.6 pcf.	138.6 pcf.	14.4%
4	1430.3	146.5	139.5 pcf. at 4 1/2" in- to hwy slab	5.0%
5	1343.0	153.1	139.5 pcf.	9.7%
6	1339.3	153.4 pcf.	136.5 pcf. at 6 1/2" in- to hwy slab	12.4%
7	1404.7	148.4 pcf.	136.5 pcf.	8.7%

TABLE A-2

CORE SAMPLE DATA USING CORE 43 + 75 AS STANDARD

I (core 43 + 75 standard) = 1351.4 c/m
 I_0 (no absorber) = 5794.3 c/m
 ρ (average density of concrete at 43 + 75) = 2.215 g/cm³
 μ_m (mass attenuation coefficient) = 0.657 cm²/g
 t = 10 cm
 conversion factor = 62.43 pcf./g/cm³

Core Sample 44 + 25

inches down core	counts/min	average core density from manual scan	corresponding field measured density	% difference in density
1	1347.0	138.6 pcf.	(no data)	
2	1319.0	140.6 pcf.	" "	
3	1358.5	137.8 pcf.	" "	
4	1347.0	138.6 pcf.	143.2 pcf. at 4 1/2" in- to hwy slab	3.2%
5	1301.7	141.9 pcf.	143.2 pcf.	0.9%
6	1274.0	143.9 pcf.	142.7 pcf. at 6 1/2" in- to hwy slab	0.8%
7	1315.5	140.9 pcf.	142.7 pcf.	1.3%

Rotated Core 44 + 25 by 90°

1	1343.0	138.9 pcf.	(no data)	
2	1302.3	141.8 pcf.	" "	
3	1307.3	141.5 pcf.	" "	
4	1368.5	137.1 pcf.	143.2 pcf. at 4 1/2" in- to hwy slab	4.3%
5	1247.5	145.9 pcf.	143.2 pcf.	1.9%
6	1244.0	145.2 pcf.	142.7 pcf. at 6 1/2" in- to hwy slab	2.5%
7	1379.0	136.4 pcf.	142.7 pcf.	4.4%

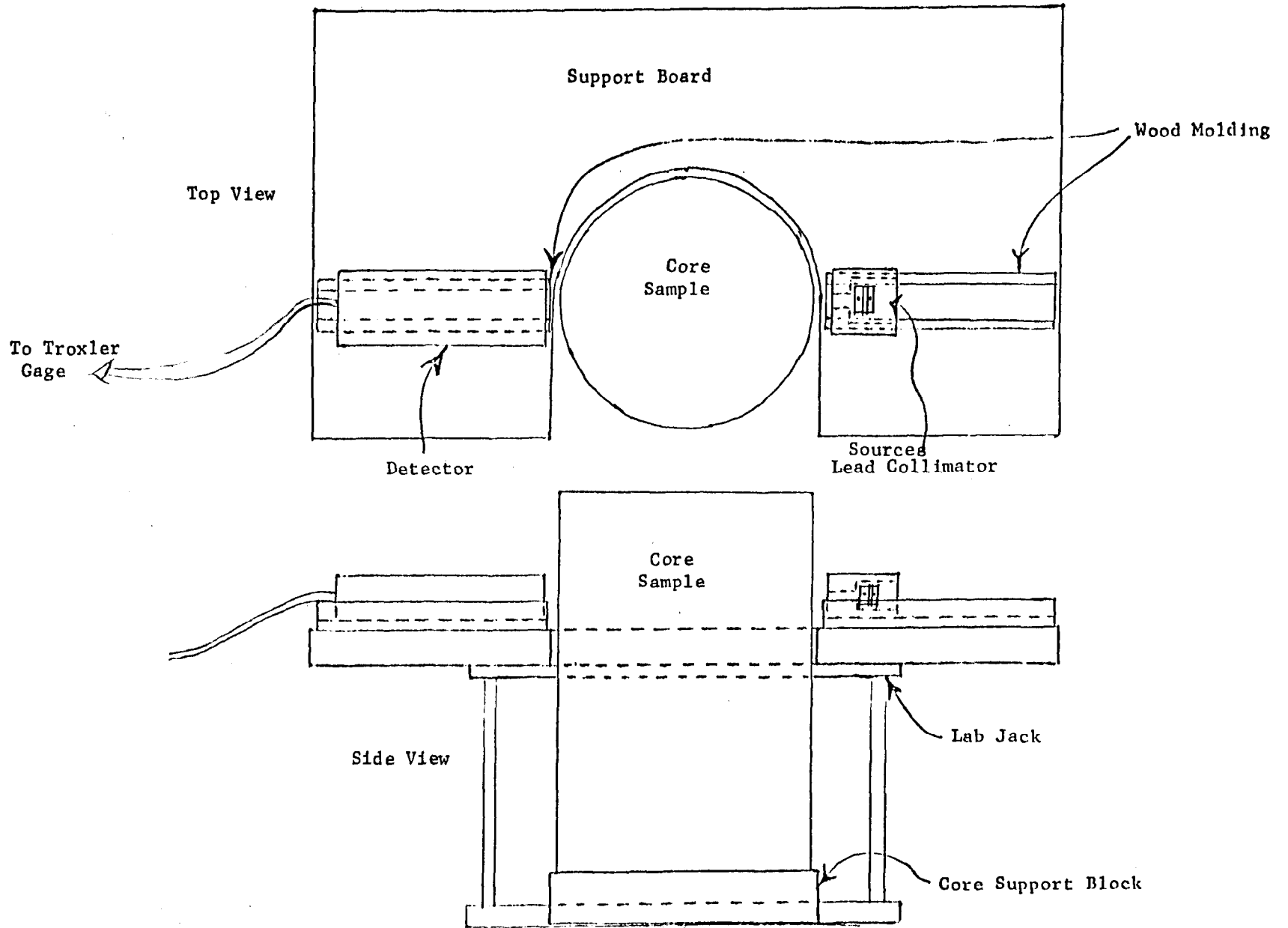
TABLE A-2 Cont'd.

Core Sample 44 + 100				
inches down core	counts/ min	average core density from manual scan	corresponding field measured density	% difference in density
1	1457.5	131.1 pcf.	(no data)	
2	1373.5	135.8 pcf.	138.6 pcf. at 2 1/2" in- to hwy slab	1.3%
3	1333.0	138.6 pcf.	138.6 pcf.	0.7%
4	1255.5	145.3 pcf.	142.5 pcf. at 4 1/2" in- to hwy slab	1.9%
5	1266.0	144.5 pcf.	142.6 pcf.	1.3%
6	1358.0	137.9 pcf.	140.0 pcf. at 6 1/2" in- to hwy slab	1.5%
7	1339.0	139.2 pcf.	140.0 pcf.	0.6%

Rotated Core 44 + 100 by 90°

1	1407.0	134.5 pcf.	(no data)	
2	1392.5	135.5 pcf.	138.6 pcf. at 2 1/2" in- to hwy slab	2.2%
3	1285.0	143.1 pcf.	138.6 pcf.	3.2%
4	1252.0	145.6 pcf.	142.6 pcf. at 4 1/2" in- to hwy slab	2.1%
5	1370.5	137.0 pcf.	142.6 pcf.	3.9%
6	1348.5	138.5 pcf.	140.0 pcf. at 6 1/2" in- to hwy slab	1.1%
7	1249.0	145.8 pcf.	140.0 pcf.	4.1%

CORE SAMPLE SCANNER



69

Figure A-1

Automatic Scanner

While the manual scan of the core sample provided good information, it was time consuming and there was always the possibility that voids located between the measurement points, 1 inch apart, could be missed.

The automatic scanner used a 2 foot by 5/8 inch diameter threaded steel rod which was coupled to the shaft of a 12 volt motor with gear speed reduction by means of a rubber coupling to allow for misalignment and flexing. The shaft was supported by two plastic bearings manufactured from p.v.c. pipe and polyethylene plastic tubing. The cradle that holds the core itself was constructed from a piece of extruded 1/8 inch aluminum channel 4 by 8 inches, which had been drilled and tapped for four small wheels. The cradle assembly was then drilled and bolted to the two drive nuts on the drive shaft. This formed the carrier assembly. A set of tracks made from 1 inch by 1 inch boxed beams and angle iron served to provide a smooth level surface for the cradle to roll on. This frame was also drilled and centered to support the drive shaft bearings. All of the above sub-assemblies were mounted on a piece of 1/4 inch by 9 1/2 inches by 32 1/2 inches plywood. The plywood base provides the needed rigidity and alignment necessary to make the sub-assemblies function together as a single mechanism.

The entire system was tested and then disassembled for painting and lubricating, then reassembled and a double throw control switch was wired to the motor. The switch controlled the forward, reverse, and on-off modes of the motor's operation. An automobile battery provides the 12 volts needed to run the motor.

Figure A-2 is a sketch of the core transport mechanism. The NaI(Tl) detector and Cs-137 sources were collimated to pass a thin beam of gamma rays through the diameter of the core sample as it was transported passed the beam. A strip chart recording of the radiation intensity was produced. A 100 μ Ci Cs-137 source provided sufficient gammas to make rapid, sensitive scans. Larger sources could have improved sensitivity still further. Figure A-3 is a typical plot of the scan of a core. No large voids were detected.

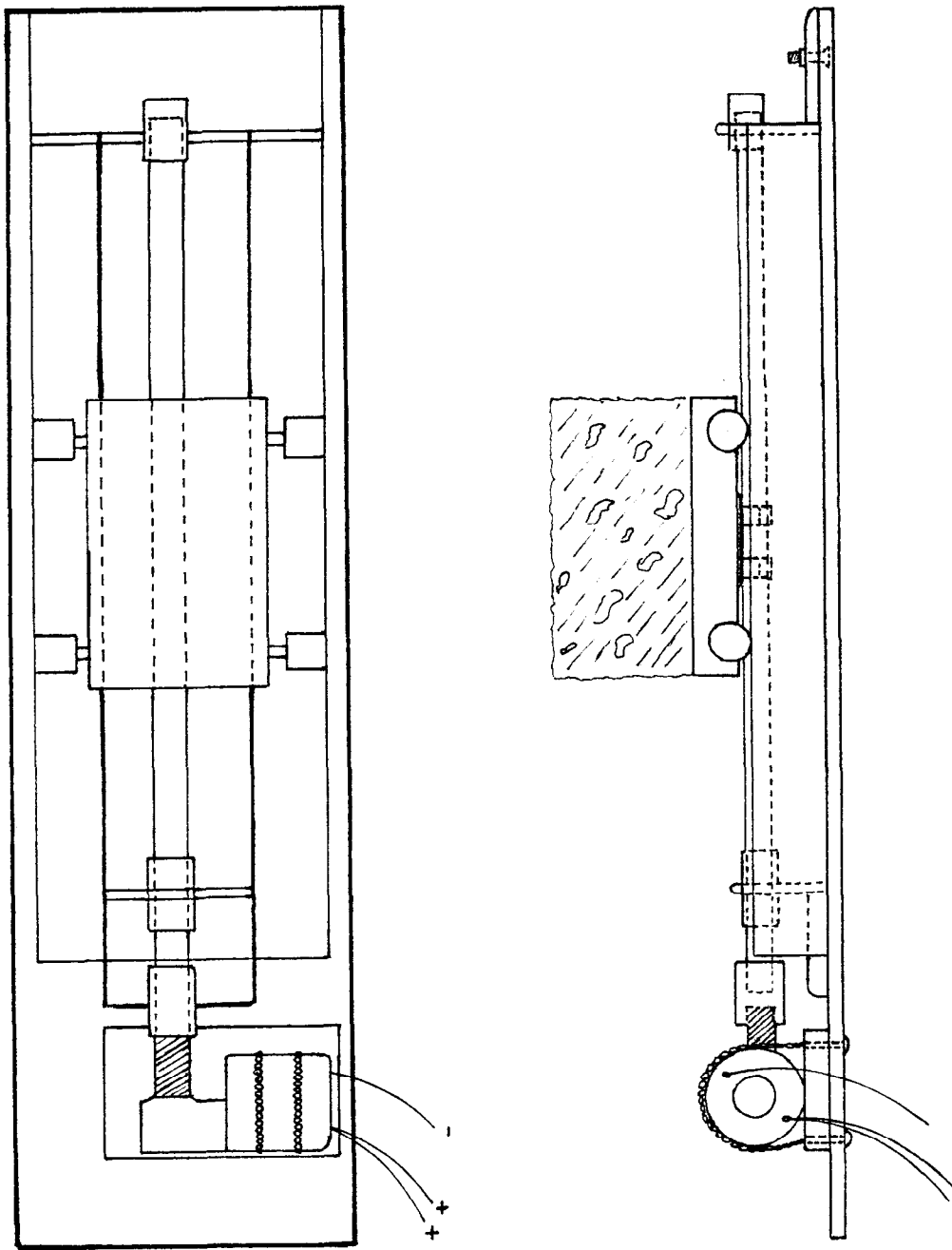


Figure A-2

Core Sample 43 + 75
Run #6
Collimated 100 μCi ^{137}Cs
Collimated NaI detector
Rotated 90°

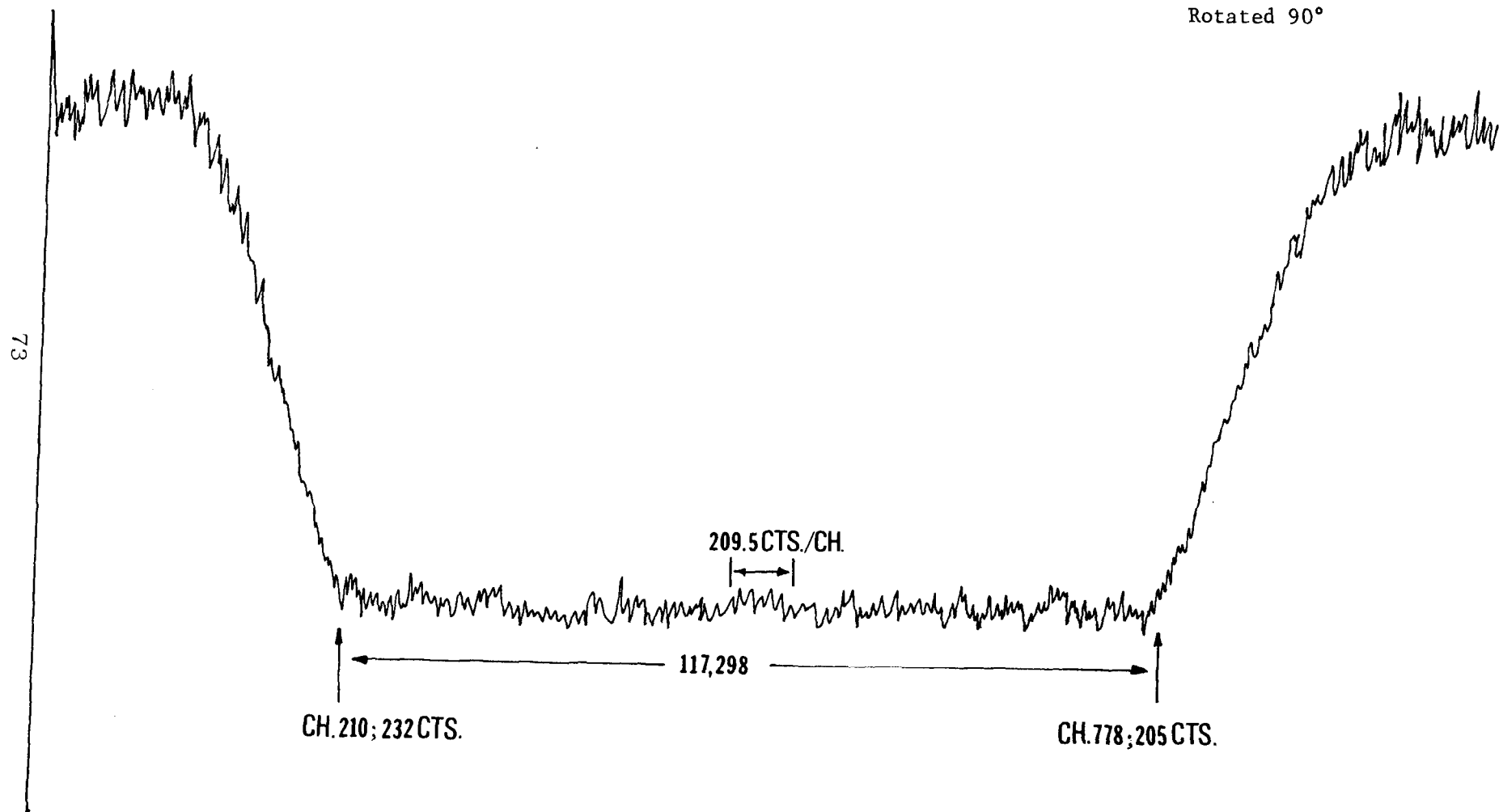


Figure A-3

APPENDIX B

Table 1B

FIELD DENSITY RESULTS

PROJECT A

<u>STATION</u>	<u>DEPTH(inches)</u>	<u>DENSITY(lbs./cu.ft.)</u>	<u>REMARKS</u>
192+00	2.25	146.9	
	4.25	147.6	
189+50	1.25	149.7	possible surface influence
	3.25	145.1	
	5.25	143.6	
189+00	2.75	145.1	
	4.75	145.9	
188+60	1.25	146.3	
	3.25	144.4	
	5.25	145.1	
188+10	2.75	147.3	slump test = 3"
	4.75	146.8	
187+50	2.75	146.0	rodded unit weights = 145.6 and 146.0 lbs/cu.ft.
	4.75	146.0	
187+00	2.25	146.5	slump test = 2.5"
	4.25	145.5	
185+75	1.25	146.0	
	2.25	146.6	
	4.25	146.0	
185+25	1.25	147.7	
	3.25	146.0	
	5.25	144.8	
184+75	1.25	148.6	possible surface influence
	3.25	146.5	
	5.25	147.8	

Table 2B

FIELD DENSITY RESULTS

PROJECT B

<u>DEPTH</u>	<u>STA.267+92</u>	<u>STA.268+88</u>	<u>STA.270+48</u>	<u>STA.275+10</u>	<u>STA.276+95</u>
1.25	135.8	137.1	141.0	133.0	137.3
2.25	133.5	140.4	139.7	139.2	138.1
4.25	138.1	133.2	135.1	138.4	138.2
6.25	136.5	136.2	138.5	139.0	138.1

76

<u>DEPTH</u>	<u>STA.279+31</u>	<u>STA.280+84</u>	<u>STA.283+95</u>	<u>STA.285+92</u>	<u>STA.292+05</u>	<u>STA.293+90</u>
1.25	137.8	141.6	142.1	143.5	139.7	141.5
2.25	138.5	142.1	144.4	141.3	140.9	140.3
4.25	136.9	143.4	141.2	141.6	137.5	138.8
6.25	136.9	144.4	142.0	139.2	135.5	141.6

REMARKS:

All depths are relative to pavement surface and are in inches. Densities at stations indicated are in lbs./cu.ft.
 Rodded unit weights taken at stations 270+40 = 141.1 lbs./cu.ft. and 285+90 = 143.1 lbs./cu.ft.
 Tests taken over a two day period with problems with water content at batch plant occurring.
 Batches were either very dry or very wet (6" slump). Cores taken later showed honeycomb structure at some stations.

Table 3B

FIELD DENSITY RESULTS

PROJECT C

<u>STATION</u>	<u>DEPTH (inches)</u>	<u>DENSITY (lbs./cu.ft.)</u>	<u>REMARKS</u>
115+36	1.31	141.2	
	3.31	142.4	
	5.31	141.5	
116+00	1.81	139.6	
	3.81	142.9	
	5.81	142.5	
118+40	1.1	142.2	Rodded unit weight= 142.3 lbs./cu.ft.
	3.1	142.9	
	5.1	139.7	
119+00	1.6	135.9	
	3.6	141.7	
	5.6	142.0	
119+75	2.1	140.1	
	4.1	138.3	
	6.1	137.5	
120+25	1.8	140.5	
	3.8	140.4	
	5.8	141.4	

Table 4B

FIELD DENSITY RESULTS

PROJECT D

<u>STATION</u>	<u>DEPTH (inches)</u>	<u>DENSITY (lbs./cu.ft.)</u>	<u>REMARKS</u>
131+50	1.9	144.4	
	3.9	142.8	
	5.9	144.4	
132+00	2.7	143.8	
	4.7	142.8	
	6.7	143.9	
133+00	1.7	142.9	
	3.7	144.7	
	5.7	144.1	
133+50	1.7	143.9	
	3.7	142.8	
	5.7	142.6	
127+50	1.4	142.4	
	3.4	142.6	
	5.4	140.3	
128+00	1.4	143.1	
	3.7	140.5	
	5.7	142.4	
129+00	1.7	143.5	Rodded unit weight=
	3.7	141.5	145.1 l lbs./cu.ft.
	5.7	142.4	Slump test= 4 in.

Table 5B

FIELD DENSITY RESULTS

PROJECT D

<u>STATION</u>	<u>DEPTH (inches)</u>	<u>DENSITY (lbs./cu.ft.)</u>	<u>REMARKS</u>
146+25	1.3	147.4	
	3.3	144.5	
	5.3	145.2	
148+00	0.8	146.5	Rodded unit weight= 144.3 lbs./cu.ft.
	2.8	144.3	
	4.8	143.4	
150+00	1.6	145.2	
	3.6	145.2	
	5.6	145.0	
150+73	1.1	146.8	Taken @ 10.5' Rt. L
	3.1	145.0	
	5.1	144.3	
150+73	0.8	146.9	Taken @ 2.5' Rt. L
	2.8	145.7	
	4.8	145.1	

Table 6B

FIELD DENSITY RESULTS

PROJECT E

<u>STATION</u>	<u>DEPTH (inches)</u>	<u>DENSITY (lbs./cu.ft.)</u>
105+20	1.25	145.4
	2.25	146.1
	3.25	143.5
	5.25	144.5
	7.25	145.3
	8.25	165.5*
105+24	1.75	155.1*
	2.75	148.6*
	3.75	145.0
	4.75	145.3
	5.75	144.7
	6.75	142.0
	7.75	150.6*
	8.75	150.3*
105+40	1.75	142.3
	3.75	148.8*
	5.75	145.2
	7.75	146.4
	8.75	157.4*

REMARKS: Approach slab steel reinforcement at approx. 2 and 8 in. from surface. Thickness of slab = 10 inches.

* Steel reinforcement affecting nuclear results. Cores at stations verified approximate steel location.

Table 7B

FIELD DENSITY RESULTS

PROJECT F

<u>STATION</u>	<u>DEPTH (inches)</u>	<u>DENSITY (lbs./cu.ft.)</u>
77+85	1.3	136.4
	2.3	152.4*
	3.3	136.6
	4.3	137.7
78+09	1.3	140.5
	2.3	154.3*
	3.3	139.5
	4.3	139.5
78+29	1.3	139.5
	2.3	140.2
	3.3	141.1
	4.3	139.3

REMARKS: Rodded unit weight @ STA.78+29 = 137.0 lbs./cu.ft.
 One man vibrating in test areas with spud vibrator.
 Rebar 2" (horizontal) from detector probe between
 detector & source @ STA.77+85. Rebar 2" (horizontal)
 from source probe between detector & source @ STA.78+09.
 Top layer of steel approx. 2" from surface. Bridge slab
 thickness = 8".

Table 8B

FIELD DENSITY RESULTS

PROJECT G
(SPAN #1)

<u>STATION</u>	<u>DEPTH (inches)</u>	<u>DENSITY (lbs./cu.ft.)</u>
105+78	1.8	140.0
	2.8	139.1
	3.8	148.3*
	4.8	140.6
	5.8	142.5
106+24	1.3	142.1
	2.3	140.1
	3.3	141.0
	4.3	144.0*
	5.3	142.2

REMARKS: Rodded unit weight @ STA.106+24 = 142.5 lbs./cu.ft.
Center of top & bottom rebars approx. 2.75" & 6.4",
respectively, from surface. Vibrating of concrete was
done manually with spud vibrator.

* Nuclear readings affected by rebars for curb & railings.

Table 9B

FIELD DENSITY RESULTS

PROJECT G
(SPAN #2)

<u>STATION</u>	<u>DEPTH (inches)</u>	<u>DENSITY (lbs./cu.ft.)</u>	<u>REMARKS</u>
106+75	0.8	141.5	Rodded unit weight=
	2.8	139.2	140.9 lbs./cu.ft.
	4.8	140.0	test location Lt. L
106+75	2.3	138.0	Rodded unit weight=
	4.3	134.0	138.6 lbs./cu.ft.
	6.3	149.2*	
106+68	1.3	128.5	
	3.3	156.7**	
	5.3	137.5	
106+28	1.6	134.5	
	3.6	138.6	
	5.6	136.5	

* Nuclear reading affect by bottom layer of steel rebars.

** Nuclear reading affect by steel rebar of curb & railings.